Quaternary Research 83 (2015) 531–544

Contents lists available at ScienceDirect

Quaternary Research

journal homepage: www.elsevier.com/locate/yqres

Reconstruction of late Quaternary paleohydrologic conditions in southeastern British Columbia using visible derivative spectroscopy of Cleland Lake sediment

Lorita N. Mihindukulasooriya [a,*], Joseph D. Ortiz [a], David P. Pompeani [b], Byron A. Steinman [c], Mark B. Abbott [b]

[a] Department of Geology, Kent State University, Kent, OH, USA
[b] Department of Geology and Planetary Science, University of Pittsburgh, Pittsburgh, PA, USA
[c] Department of Earth and Environmental Sciences and Large Lakes Observatory, University of Minnesota, Duluth, MN, USA

ARTICLE INFO

Article history:
Received 18 March 2014
Available online 24 March 2015

Keywords:
Visible derivative spectroscopy
Productivity
Lake level
Holocene
Pigment
British Columbia

ABSTRACT

Visible derivative spectroscopy (VDS) analysis of sediment from Cleland Lake, Southeastern British Columbia provides a reconstruction of paleolimnological productivity and hydrologic change during the past 14,000 calibrated ^{14}C years before present (cal yr BP). The first five principal components (PC) of the VDS data explain 97% of the variance in the VDS data set. Four PCs correlate with standard reflectance derivative spectra for diatom, dinoflagellate algae, and cyanophyte pigments that record ecological change, while two PCs are paleohydrologic indicators. Dinoflagellate algae are predominant from 11,600 to 8600 cal yr BP then decrease to low levels after ~8500 cal yr BP. PCs 3–5 represent variations in cyanophyte abundance and exhibit peaks from 14,000 to 11,600, 14,000 to 9500, and 6100 to 5400 cal yr BP, respectively. Conditions shifted toward favoring diatoms around 9400 and lasted until 170 cal yr BP. Higher dinoflagellate-related pigment concentrations suggest a lower lake level from 11,600 to 8600 cal yr BP, followed by higher water levels and wetter conditions after 8500 cal yr BP. We propose that drier conditions transitioning from the late glacial into the Holocene were caused by summer insolation-driven, non-linear feedbacks between the northern hemisphere subtropical high-pressure systems, vegetation, and soil moisture.

Introduction

Holocene climate was once thought to have been relatively stable in comparison to the dramatic changes that occurred during the late glacial period (Mayewski et al., 2004; Overpeck and Cole, 2006). However, it is now generally accepted that substantial climate variability occurred during the Holocene over years to decades, time scales important to humans (e.g. Alley et al., 2003). Such abrupt events cannot be resolved using the relatively short instrumental climate records. Therefore it is imperative to study longer, highly resolved climate proxies such as those attainable from lake sediment.

In western North America large droughts similar to those of the 2002–2004 were a common occurrence during the 20th century (Cook et al., 2004). Studies of paleoclimate proxy data have revealed that more intense droughts of longer duration occurred in the desert Southwest during the Medieval Warm Period (~900 to 1300 AD) (Cook et al., 2004, 2010). Multi-decadal drought variability in western North America is largely attributable to Pacific ocean–atmosphere dynamics involving the El Niño southern Oscillation (ENSO) and the Pacific Decadal Oscillation (PDO) (Mann et al., 2005; McCabe et al., 2004; Nelson et al., 2011; Steinman et al., 2012), as well as the teleconnected influence of the Atlantic Multidecadal Oscillation (AMO) and the North Atlantic Oscillation (NAO) (Cook et al., 2004; McCabe et al., 2004). Although drought variability during recent centuries is relatively well understood (Cook et al., 2004; McCabe et al., 2004; Steinman et al., 2014), the frequency, duration, and forcing mechanisms of hydroclimate variations on centennial to millennial time scales are poorly defined, particularly during the Pleistocene–Holocene transition (Galloway et al., 2011).

In semi-arid regions, small, closed-basin lakes are sensitive to changes in regional precipitation/evaporation (P/E) balance resulting from climate change. In these lakes, variability in P/E balance produces hydrologic instability, inducing changes in water level that can be recorded in the physical, biological, and chemical composition of sediment accumulating in the basin (Talbot, 1990; Battarbee, 2000; Leng and Marshall, 2004: Steinman et al., 2010a,b; Pompeani et al., 2012). Large-magnitude water-level variations resulting from non-linear responses to climate system feedbacks can give rise to changes in sediment characteristics (Fritz, 2008). Previous work has demonstrated that spectral reflectance, particularly visible derivative spectroscopy (VDS), is an efficient and non-destructive method of quantitatively analyzing

* Corresponding author.
E-mail address: lmihindu@kent.edu (L.N. Mihindukulasooriya).

http://dx.doi.org/10.1016/j.yqres.2015.02.003
0033-5894/

organic matter content (including plant pigments), clays, carbonates, and iron oxides in sediment to reconstruct paleoclimate (Ortiz et al., 1999, 2009, 2012).

Fossil pigments are an important constituent of the organic matter preserved in lake sediment and can be used as a proxy for primary productivity and changes in phytoplankton community structure within lakes (Bouchard et al., 2013; Das et al., 2005; Peteet et al., 2003; Wolfe et al., 2006). Concentrations of sedimentary photosynthetic pigments have long been used as a direct and accurate method for reconstructing the response of lake phytoplankton to environmental changes (Nara et al., 2005; Sanger, 1988; Sanger and Crowl, 1979; Sanger and Gorham, 1972). Ecological succession, which occurs on a variety of time scales, is a well known principle by which community structure changes in an essentially orderly fashion in response to stochastic factors and external or internal stimuli (Connell and Slatyer, 1977; Peet and Christensen, 1980; Pickett et al., 1987). In addition to the earliest definition of succession, as the sequential changes in species, latter studies have described succession in terms of changes in characteristics such as biomass, productivity, diversity, and niche breadth (Connell and Slatyer, 1977; Wilson, 1994; Müller-Navarra et al., 1997). Phytoplankton composition in temperate lakes tends to follow a succession pattern similar to that of plants on the landscape and is strongly influenced by water chemistry and lake level (Müller-Navarra et al., 1997). Biological communities in drought-sensitive lakes are therefore a reflection of water-balance changes, such that algal pigment analysis of sediment from these lakes can be used to investigate past hydroclimate variability and community succession. To this end we present the progression of phytoplankton communities at Cleland Lake, an alkaline, surficial, closed-basin lake in southeastern British Columbia, using VDS analysis of lake sediment cores. A major objective of this paper is to validate the use of VDS methods in paleolimnological and paleoclimatic reconstructions. A secondary objective is to understand the timing and magnitude of regional environmental change, particularly during the late Pleistocene and early Holocene by reconstructing paleo-lake productivity and hydrologic balance variations.

Study area

Cleland Lake (50.82° N, 116.38° W, 1158 m) is located in the north–south trending Columbia Valley just west of the continental divide in the Rocky Mountains of southeastern British Columbia (Fig. 1). The lake has a surface area of 23.5 ha (0.235 km^2), a maximum depth of 31.7 m and is typically covered with ice from November to May. The surface inflow is limited to the relatively small, immediate catchment, while water losses are restricted to evaporation and (presumably) some groundwater seepage.

Present climate of Southeastern British Columbia

The climate of British Columbia is strongly influenced by sea surface temperature (SST) and atmospheric circulation over the Pacific Ocean (Moore et al., 2010). The north–south trending mountain ranges in the region restrict the east–west flow of the seasonably variable winds (Moore et al., 2010). The dominant modes of inter-annual to inter-decadal atmosphere–ocean variability affecting British Columbia include: ENSO, PDO, the Pacific North American Pattern (PNA), and Arctic Oscillation (AO) (Moore et al., 2010). El-Niño winters in British Columbia are warmer and drier than normal, while La-Niña winters are cooler and wetter (Moore et al., 2010). The positive phase of the PNA is characterized by a strong Aleutian Low and a high pressure ridge over the Rocky Mountains, resulting in warm, dry winters in British Columbia and vice versa (Moore et al., 2010).

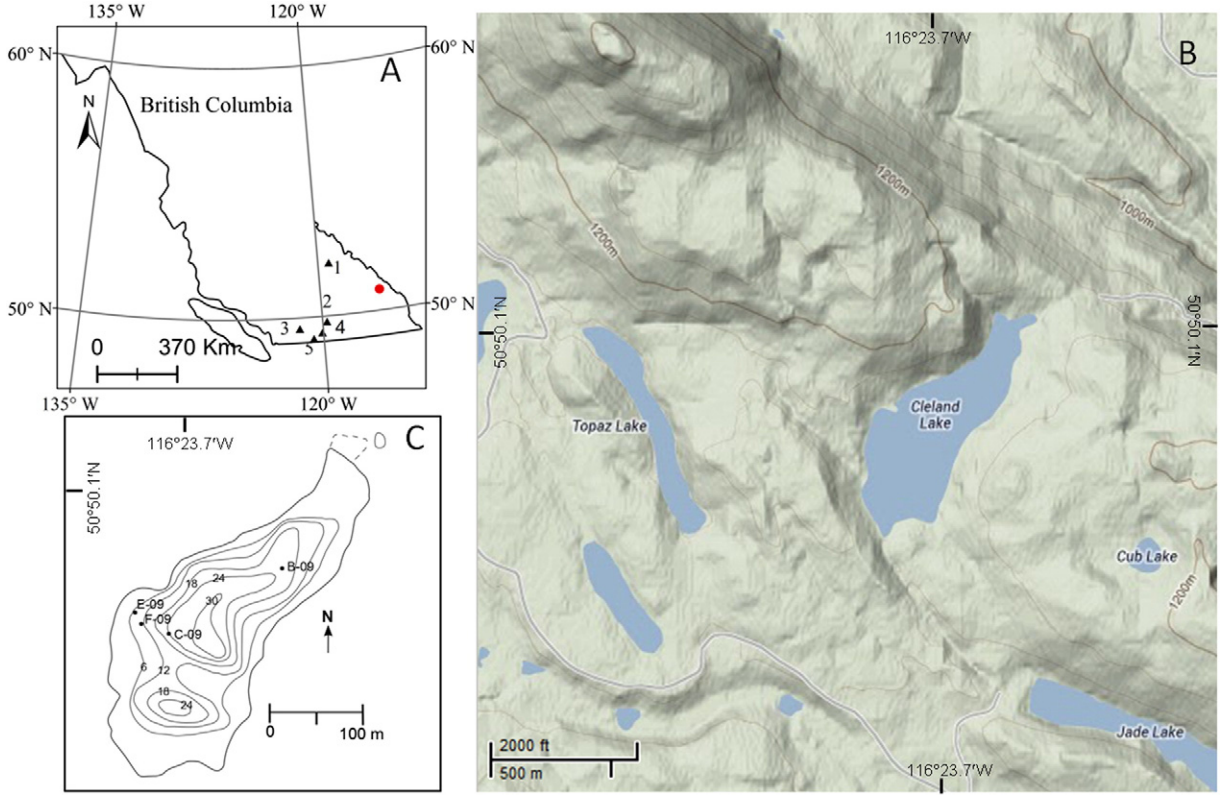

Figure 1. Cleland lake location map. A. Map of British Columbia showing the location of Cleland Lake (red dot) and selected sites referenced in the text (black triangles), 1: Eleanor Lake, 2: Windy Lake, 3: Frozen Lake, 4: North Crater Lake, 5: Lake of the Woods. B. Topographical map of watersheds in the Cleland Lake locale. C. Bathymetry map of Cleland Lake, showing the locations of core sites.

Cleland Lake is located within the Columbia Mountains and southern Rocky Mountains Physiographic region and the Interior Douglas-fir Biogeoclimatic zone (Moore et al., 2010). This interior region has relatively low precipitation during spring, but wet early summers (Moore et al., 2010). Data from Meteorological Services of Canada's Brisco weather station (ID 1171020, 10 km east of the lake, elevation 823 m) documents a mean annual temperature of 11.2°C over the period from 1984 to 2003 AD (Fig. 2A). January mean temperature was −3.7°C and the July mean temperature was 24.8°C. Mean annual precipitation was 428 mm with 30% of that received as snowfall. The mean annual rainfall during the period from 1924 to 2003 AD was 302 mm with 70% of the rainfall occurring during the summer months (May to September).

Methods

Sediment core collection

Four sediment cores (B-09, C-09, E-09, and F-09) were collected from Cleland Lake in May and July 2009. Cores E-09 and F-09 were collected at water depths of 7.0 m and 12.8 m, respectively, while cores B-09 and C-09 were collected at water depths of 20.2 m and 24.0 m (Fig. 1A). The uppermost sediment depth of cores B-09, E-09, and F-09 is 30 cm below the sediment water interface. Cores E-09 and F-09 were collected using a square rod-driven, Livingston piston corer. Core B-09 (deep water) is 2.5 m long and was collected with a rod-driven, polycarbonate piston corer. Core C-09 was recovered from a water depth of 24 m using a freeze corer filled with a mixture of ethanol and dry ice. The shallow water core E-09 consists of four overlapping drives extending to a sediment depth of 2.6 m. The intermediate water core F-09 consists of six overlapping drives that extend 3.3 m below the sediment–water interface. Core drive overlaps were identified by visual examination of sedimentological features. Individual Livingston core drives were wrapped in clear polyvinyl plastic and sealed in PVC casing in the field. All cores were transported to the Department of Geology and Planetary Science at the University of Pittsburgh. The Livingston and polycarbonate cores were stored at 4°C, while the freeze core was stored at −10°C prior to sampling and analysis. Water temperature, pH, dissolved oxygen, conductivity, and alkalinity were measured using a Hach® Hydrolab water quality sonde and Hach® Digital Titrator.

Geochronology

Bulk sediment samples were digested in 7% H_2O_2 for ~12 h and sieved at 63 μm. Terrestrial macrofossils (>63 μm) were picked using a small brush under a binocular light microscope for radiocarbon dating. Samples were treated with an acid–base-acid wash and rinsed with deionized water to neutral pH prior to being analyzed at the W.M. Keck Carbon Cycle Accelerator Mass Spectrometry Laboratory at the University of California, Irvine (UCI) as described in Abbott and Stafford (1996). The F-09 core chronology is based on four AMS ^{14}C dates on terrestrial macrofossils and two tephra layers of known age (Table 1). A linear point-to-point age model was generated using the CLAM 1.0.2 software with the IntCal09 calibration curve (Blaauw, 2010; Reimer et al., 2009). The basal age was extrapolated following the trend established by the two oldest age model control points (Fig. 3, Table 1). The "best" age estimates for the CLAM age model are generated by Monte Carlo simulation of the multi-modal ^{14}C calibration age distributions using a non-normalized, two standard deviation calibration range as opposed to a simple, Gaussian distribution (Blaauw, 2010). The CLAM calibration software then produces an age model by calculating the age estimates and 95% confidence intervals for each depth in-between individual dated depths (Blaauw, 2010). However, comparison of the age model estimates from CLAM 1.0.2 calibration with CALIB 6.0 calibration methods indicates that, there were no significant differences between the two methods that we generated for comparison for this data set (Supplementary Table 1).

Visible derivative spectroscopy

Visible derivative spectroscopy is a quantitative, non-destructive method of sediment analysis. Diffuse spectral reflectance was measured at 0.5 cm intervals on the wet, split-core sediment surface of cores B-09, E-09, and F-09 using a handheld Minolta CM-2600d spectrophotometer (Konica-Minolta USA, Ramsey, NJ, USA). This instrument measures the reflectance over the visible range of the electromagnetic spectrum (380–700 nm) at 10 nm resolution. Sediment reflectance of the dried,

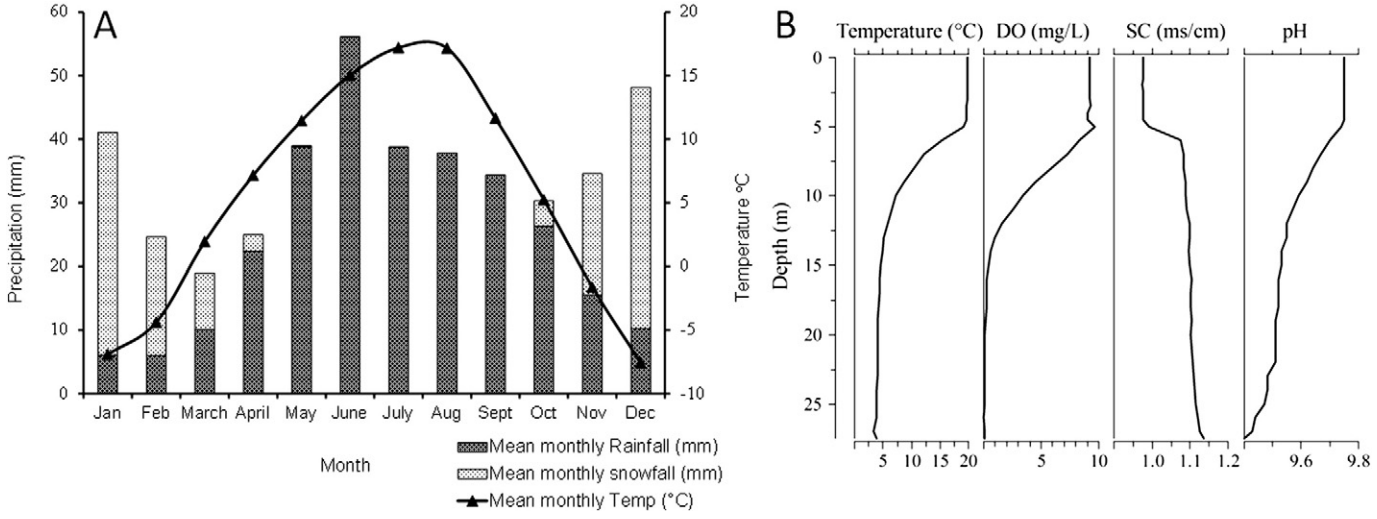

Figure 2. A. Annual cycle of temperature and precipitation in Brisco, BC (10 km from Cleland Lake). Mean monthly precipitation is the average from AD 1924 to 2003 and the mean monthly temperature (black triangles) is the average from AD 1984 to 2003. B. Limnological measurements of the Cleland Lake water column on July 2011: temperature (T), dissolved oxygen (DO), specific conductivity (SC), and pH.

Table 1
AMS radiocarbon and tephra dates for Cleland Lake core F-09.

UCAIMS No.	Material	Core depth (cm)	^{14}C yr BP	Median calibrated age (cal yr BP)	2σ lower (cal yr BP)	2σ upper (cal yr BP)
84885	Charcoal	35.5	210 ± 80	200	−10	430
	Mt. St. Helens tephra layer	66.5		480	470	490
84851	Charcoal	162.5	3660 ± 20	4000	3920	4100
	Mazama tephra layer	204–208	6850 ± 100	7700	74,540	7920
84852	Charcoal	214	7435 ± 30	8100	8030	8280
99884	Charcoal	286	9800 ± 350	11,300	10,280	12,390
	Extrapolated basal age	357.5	N/A	14,100	12,800	15,480
84886	Charcoal	287	780 ± 20*	700	680	730

* Outlier radiocarbon age omitted from the age model.

freeze core samples from C-09 was measured using an ASD LabSpec Pro FR UV/VIS/NIR spectrometer equipped with a high-intensity contact probe. This instrument measures diffuse reflectance over the visible and near infrared range of the electromagnetic spectrum (350–2500 nm) at ~4 nm resolution in the visible and 10 nm resolution in the near infrared (NIR). The resulting spectrum was band-averaged to 10 nm reflectance for direct comparison with the Minolta data. We analyzed data in the visible range (400–700 nm) to avoid noise in the ultraviolet (UV) and differences in the reflectance and absorption processes in the NIR relative to the visible (Ortiz, 2011). The measured reflectance of the powered samples was empirically adjusted for the increased reflectance of dried relative to moist samples by multiplying each spectrum by a constant scaling factor of 0.5. This conversion enables direct comparison of the ASD measurements of the dried samples with the Minolta measurements generated from moist sediment (Fig. 4).

Visible derivative spectroscopy (VDS) was used to define sediment pigment content based on the shape of components extracted from the center-weighted derivative of the diffuse spectral reflectance (DSR) spectra measured at each depth. The center-weighted derivative spectrum measures the rate of change of reflectance as a function of wavelength and was calculated numerically as: $\partial R_i/\partial\lambda_i = (R_{i+1} - R_{i-1})/(\lambda_{i+1} - \lambda_{i-1})$, where R is the reflectance for a given 10 nm band in the spectrum, λ is the wavelength and i represents the index of the appropriate element (Brenner, 2014; Ortiz, 2011).

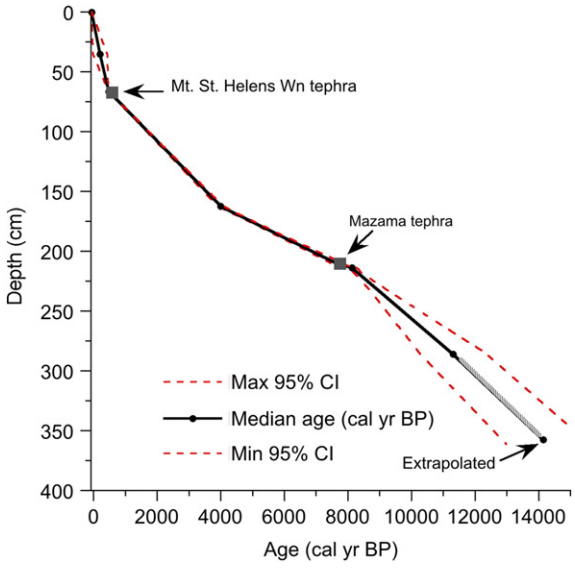

Figure 3. Age vs. depth model of Cleland core F-09 (0 to 361.5 cm) based on four radiocarbon dates and two tephra layers. Red dotted lines represent the 95% confidence interval.

Principal component analysis

Varimax-rotated, principal component analysis (VPCA) of the correlation matrix derived from the center-weighted derivative of the DSR data extracts orthogonal components that can be related to sediment composition (Ortiz, 2011; Ortiz et al., 2009; Yurco et al., 2010). The derivative transformation minimizes scattering effects, which influence the raw reflectance spectral shape. VPCA was conducted in SPSS™ 14.0 using the full data set (1751 reflectance measurements) based on all four cores to allow comparison of results between cores. The components were identified by comparing the principal component (PC) loading spectra for each of the PCs with center-weighted reflectance derivative spectra for previously published pigments or known mineral standards in the USGS spectroscopic library or minerals measured in Ortiz' lab at Kent State University (Clark et al., 2007; Gantt, 1975; Graham and Wilcox, 2000; Ortiz, 2011; Ortiz et al., 2009; Robertson et al., 1999; Schagerl and Donabaum, 2003; Schagerl et al., 2003;

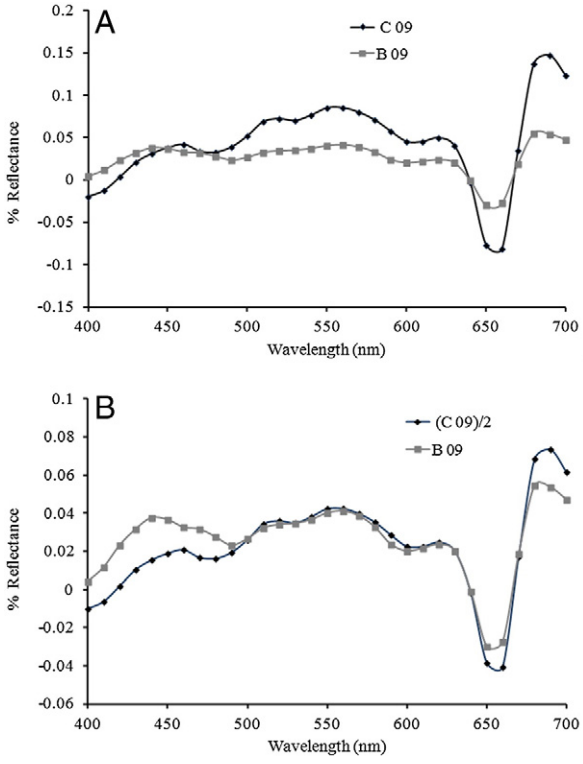

Figure 4. Adjusting reflectance of powdered samples. A. Comparison of the reflectance of a representative dry sediment sample from the core C-09 (black diamonds) with the reflectance of wet sediment sample from the deep core B-09 (gray squares). B. Adjusted reflectance of the dry sediments from the core C-09 by dividing by a factor of two.

Toepel et al., 2005; Yurco et al., 2010). We quantified the relative importance of each pigment or mineral in the PC by fitting a weighted-average of the empirically selected standards to each principal-component loading pattern. The quality of the fit was determined by linear correlation. This process is identical to the approach previously applied to marine cores (Bouchard et al., 2013; Ortiz, 2011; Ortiz et al., 2009) and similar to spectral matching methods used in X-ray Diffractometry (Eberl, 2003, 2004).

Bulk physical properties by loss on ignition and X-ray fluorescence

Organic carbon, carbonate content, and mineral matter were measured by loss on ignition (LOI) at the University of Pittsburgh, following Heiri et al. (2001). The Cleland Lake sediments were measured at 2 cm intervals for LOI. The bulk elemental composition of the lake cores was measured using the ITRAX X-ray Fluorescence (XRF) core scanner at the University of Minnesota, Duluth. The scanner has the potential to scan cores at 0.2 mm resolution and employs a Molybdenum X-ray source. The Cleland F-09 core was scanned at 5 mm resolution at 30 mA and 45 kV using a scan time of 60 s to increase the signal to noise ratio. Biogenic silica in lake sediment primarily derive from diatoms and can be related to millennial scale climatic changes (Brown, 2011; Johnson et al., 2011; Williams, 1995). Independent studies have found a strong correspondence between biogenic silica abundance derived from conventional methods and XRF derived Si:Ti ratios (Brown, 2011; Brown et al., 2007; Johnson et al., 2011). Hence Si:Ti ratios can be used as a proxy for biogenic silica abundance (Brown et al., 2007; Johnson et al., 2011).

Results

Lake limnological properties

Cleland Lake is stratified during the summer with an epilimnion depth of 5 m (Fig. 2). In August 2011 the epilimnion had mean values of 19.7°C for temperature, 9.2 mg/l for dissolved oxygen, and 9.75 for pH. The metalimnion spanned the depth range from 5 to 12 m, while the hypolimnion, which extended from 12 to 29 m depth, had a mean temperature of 5.8°C, mean dissolved oxygen concentration of 1.6 mg/l, and a mean pH of 9.5. The lake water is alkaline, with a dissolved bicarbonate and carbonate concentration of ~530 mg/l, which promotes the production of micritic calcium carbonate in the water column during warm season whiting events. The lake water is anoxic below 12 m, which reduces sediment bioturbation and aids preservation of plant pigments within sub-mm laminations.

Age model

The age model for core F-09 spans the period from 11,300 ± 1050 cal yr BP to present (Fig. 3, Table 1,). Linear extrapolation of the last two age control points yields an age of 14,100 ± 1300 cal yr BP for the base of the core. The thickness of the error envelope ranges from ±50 to ±100 yr at the top of the core, increasing up to ±200 to ±500 yr between the depths of 225 to 250 cm. Uncertainty in the basal ages increases from ±1000 cal yr BP at an age of ~11,300 cal yr BP to ±1300 cal yr BP at the base of the core.

Bulk sediment properties

Bulk properties of the core were analyzed by XRF and LOI (Fig. 5). The basal section of core F-09 (361–295 cm) consists of clayey silt. The sediment is characterized by high mineral matter (50–90%), low carbonate content (<20%), and low organic matter (<10%) (Figs. 5A, B and C). Clastic sediment transitions to well-laminated organic mud at 298 cm and extends up to 275 cm. Organic carbon and carbonate content rapidly increase after 300 cm, while the mineral content gradually

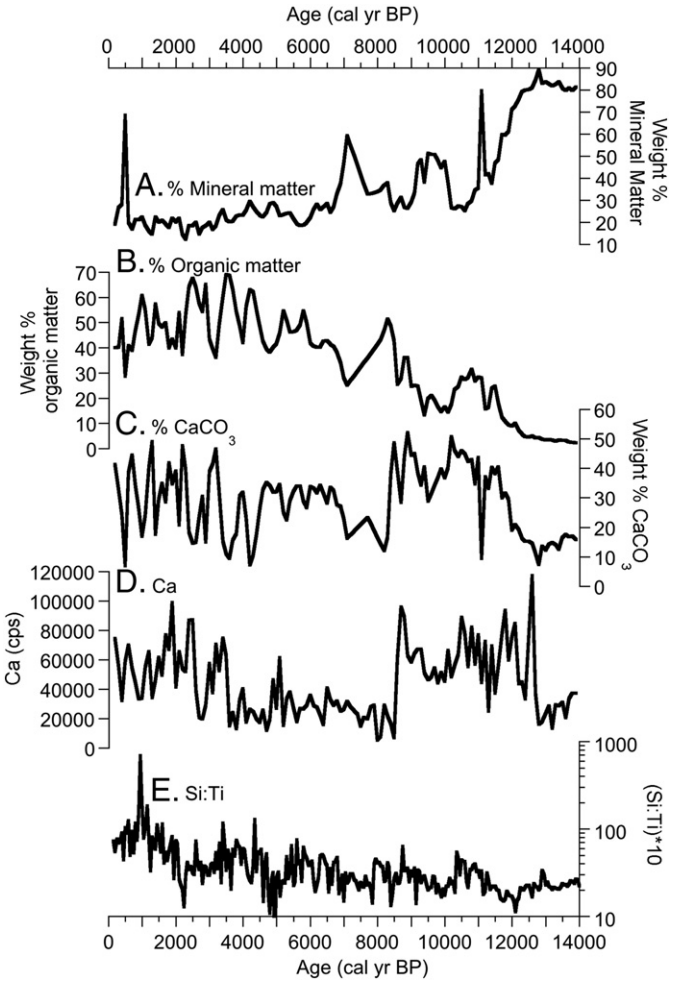

Figure 5. Bulk sediment properties of the core F-09. A. percent mineral matter content by weight, B. percent organic matter by weight, and C. percent $CaCO_3$ by weight obtained from loss on ignition. D. Ca concentrations (counts per second) obtained from XRF analysis of the intermediate depth core (F-09) E. Si:Ti ratios, plotted on a log scale to enhance the visualization of the data.

drops to lower levels. The stratigraphy transitions from being poorly laminated to massive and carbonate-rich between 290 and 227 cm. Corresponding to these depths, LOI-derived calcium carbonate percentage and XRF derived Ca concentrations rapidly rise between 307 and 290, and remain high until 225 cm (Fig. 5D). Massive to faintly laminated sediment transitions to well-laminated carbonate mud at 227 cm. Calcium carbonate content and Ca counts rapidly drop during this transition. Very finely laminated organic-rich sediment with relatively low calcium carbonate is present throughout the rest of the core (227 to 30 cm). Organic matter content gradually increases between 259 and 227 cm and remain high in the top of the core (227 to 30 cm).

The Si:Ti ratio is lower during the late glacial period (>12,000 cal yr BP), indicating low diatom abundance. The ratio gradually increases between 12,000 and 10,500 cal yr BP and rapidly decreases after 10,300 cal yr BP. The Si:Ti ratio remains low between 10,300 and 9500 cal yr BP, and the ratios gradually increase after 9500 cal yr BP until 170 cal yr BP (Fig. 5E).

Variance explained by principal components

As can be seen in data from core F-09, the reflectance spectra from the lake typically exhibit high reflectance on the red end of the spectrum, and low reflectance toward the blue end of the spectrum (Fig. 6A). The derivative of the reflectance spectra demonstrates specific bands of variability with oscillations that vary throughout the record

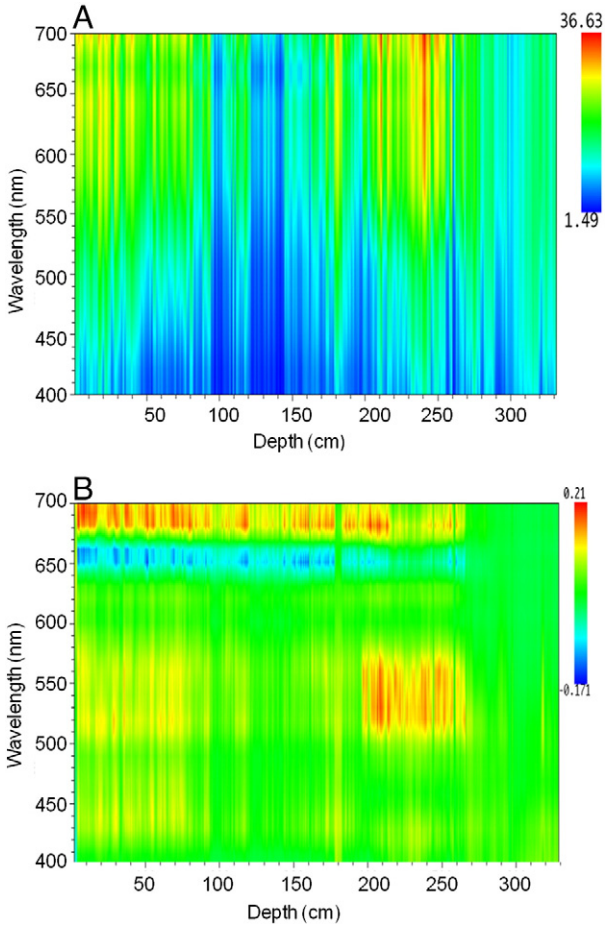

Figure 6. Spectral plot of percent reflectance of core F-09 (A) and first derivatives of the reflectance measurement of core F-09 (B). Legend to the right in plots A and B shows the range of reflectance values recoded from the samples and the center-weighted first derivatives of the reflectance between the wavelengths 400 and 700 nm respectively. Higher derivative values between the depths of 230 to 290 cm (8800–10,400 cal yr BP) and 520 to 570 nm correspond to the reflectance peak of peridinin in PC 2 and represent early Holocene peak in dinoflagaellate algae. Lower derivative values between 650 and 660 nm and higher values between 680 and 700 nm are characteristic of minimum and peak reflectance values of bacillariophyceae pigments, corresponding to diatom abundance after 230 cm (8800 cal yr BP).

(Fig. 6B). Varimax-rotated PCA was applied to the data set to partition the variability to identifiable components.

The first five PCs of the reflectance derivative data explain 97% of the variance. PC 1 explains 28% of the variance, and is interpreted as a mixture of illite (75%) and sphalerite (30%) (Table 2, Fig. 7A). PC 2 explains 24% of the variance in the reflectance derivative data and arises from a mixture of dinoflagellate algae and degradational pigments (peridinin, pheophytin-a, 60% and 33% respectively) and goethite (Table 2, Fig. 7B). PC 3 explains 23% of the variance and is a mixture of phycocyanin (80%), an accessory pigment present in cyanophytes and the clay minerals smectite and chlorite (20%, Table 2, Fig. 7C). PC 4 explains 16% of the variance and is a mixture of the spectral signatures for bacillariophycea (70%) and phycocyanin (30%) (i.e. diatom and cyanophyte photosynthetic pigments, Table 2, Fig. 7D). PC 5 explains 6% of the variance in the reflectance derivative data and is related to the cyanophyte accessory pigment, allophycocyanin (54%) and a degradation product of chlorophyll-a, the pigment pheophytin-a (46%), (Table 2, Fig. 7E).

Temporal variability of lake phytoplankton communities during the Holocene

Because core F-09 is the longest core that extends through the Holocene with reliable age control to 11,300 ± 1000 cal yr BP, we use it to study the evolution of the phytoplankton community in the lake. Variations in PCs 2–5 suggest a post-glacial succession of various classes of algae (Fig. 8). The earliest part of the record, prior to 11,800 ± 1100 cal yr BP (i.e. the deglacial period), is characterized by low diatom, cyanophyte, and dinoflagellate abundances. Dinoflagellate algal pigments record a gradual increase in abundance starting around 12,400 ± 1100 cal yr BP based on the increases in PC 2 values (Fig. 8). Dinoflagellate levels rose rapidly between 11,850 and 11,600 ± 1200 cal yr BP, reached the highest values in the record by 11,600 ± 1100 cal yr BP and remained high until 8600 ± 200 cal yr BP with excursions centered around 10,700 ± 900 and 8750 ± 400 cal yr BP. Dinoflagellate productivity remained low during the middle and late Holocene with several millennial- and centennial-scale fluctuations centered around 7500 ± 200, 6400 ± 100, 3250 ± 75, 2450 ± 50, 1550 ± 20, and 800 ± 10 cal yr BP.

PC 3 represents an early successional cyanophyte community (which we denote cyanophyte community 1), which was prominent in the lake prior to 11,600 ± 1200 cal yr BP (Fig. 8). Based on the increasing PC 3 component scores, this community rapidly decreased after 11,600 cal yr BP reaching low levels by 10,550 cal yr BP. The abundance of this community remained low throughout the rest of the record (10,500 ± 800 to 170 ± 200 cal yr BP). The early Holocene drop in cyanophyte community 1 was simultaneous with the rapid increase in dinoflagellate algae abundance inferred from PC 2. Principal component 4 represents an early successional mixed cyanophyte and diatom community (cyanophyte community 2), based on the correlation to the spectral signature for phycocyanin and bacillariophycea. The combined signature of cyanophyte and bacillariophycea in PC 2 is distinct from the spectral signature from cyanophyte community 1. The spectral signature for bacillariophycea has a positive correlation with PC 4, indicating greater diatom abundance when the PC 4 scores increase. In contrast, phycocyanin exhibits a negative correlation with PC 4, indicating lower levels of cyanophytes when PC 4 increases and vice versa. PC4 thus represents the contrasting appearance of a specific set of diatoms versus cyanophytes in cyanophyte community 2 preserved in Cleland Lake sediment. Cyanophyte community 2 appeared in the lake during the late glacial period, but remained abundant longer than cyanophyte community 1 (14,100 ± 1300 to 9500 ± 500 cal yr BP). PC 4 also indicates that diatom abundance was low prior to 11,800 ± 1200 cal yr BP, then increased rapidly during three intervals centered on 11,550, 11,400, and 11,200 ± 1200 cal yr BP (Fig. 8). Diatom levels gradually dropped to their lowest values after 11,100 ± 1000 and remain lower between 10,800 ± 700 to 9500 ± 400 cal yr BP, while the cyanophyte portion of cyanophyte community 2 levels rose to their highest

Table 2
Total variance explained by the first five components from the Principal component analysis and their correlated reference spectra.

Component	Percent of variance explained	Cumulative percent of variance explained	Correlated reference spectra	Correlation to the reference spectra
1	27.95	27.95	95% illite + 5% sphalerite	0.91
2	23.94	51.89	60% peridinin + 33% phaeophytin-a + 7% goethite	0.87
3	23.17	75.06	80% phycocyanin + 20% (smectite + chlorite)	0.86
4	16.32	91.38	70% bacillariophycea + 30% phycocyanin	0.91
5	5.7	97.08	54% allophycocynain + 46% pheophytin-a	0.78

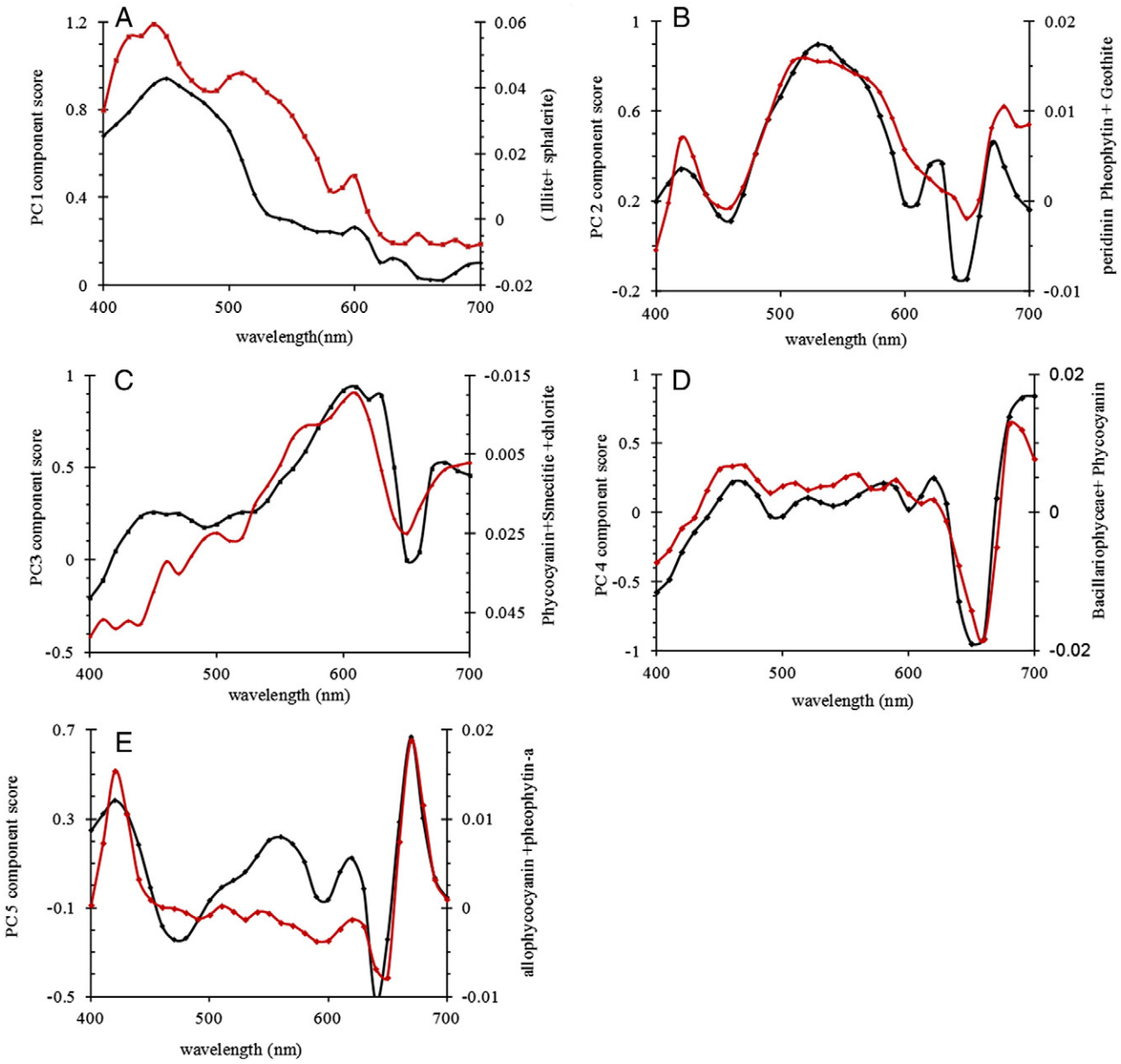

Figure 7. Comparison of first five principal components with their reference spectra. The primary y axis represents the component scores while the secondary y axis represent the first derivative of the percent reflectance of the reference spectra. Black line represents the principal component while the red line is the correlating reference spectrum for each component. PC 1 (black line) and the first derivative spectra of the 70% illite + 30% sphalerite (red line) mixture. B. PC 2 (dinoflagelltae algae scores, black line) and the first derivative spectra of the 60% peridinin + 33% phaeophytin-a + 7% goethite (red line) mixture. C. PC 3 scores (clay and cyanophytes, black line) and the first derivative spectra of the 80% phycocyanin + 20% (smectite + chlorite) mixture; (red line), D. PC 4 scores (diatoms and cyanophytes); black line and the first derivative spectra of the 70% bacillariophycea + 30% phycocyanin mixture (blue line). E. PC 5 (black line) and the first derivative spectra of the 54% allophycocynain + 46% pheophytin-a mixture (red line).

Holocene levels. Cyanophyte community 2 pigment concentrations indicate an increase in diatoms after 9500 ± 500 cal yr BP and remained high from 8500 ± 200 to 170 ± 200 cal yr BP with several millennial- and centennial-scale oscillations. Overall, diatom levels increased during the middle to late Holocene, while the cyanophyte portion of cyanophyte community 2 was smaller from 9000 ± 400 to 170 ± 200 cal yr BP.

PC 5 represents a third cyanophyte community (cyanophyte community 3), also identified through the presence of phycocyanin, that became dominant in the lake during the middle Holocene (6100 ± 100 to 5400 ± 100 cal yr BP) (Fig. 8). Low PC 5 scores suggest that, cyanophyte community 3 was low in abundance during the deglacial period, but gradually increased after 11,500 cal yr BP, then peaked during the middle Holocene. Cyanophyte community 3 gradually declined after 5400 cal yr BP, then remained low in abundance throughout the late Holocene (1850 ± 50 to 170 ± 200 cal yr BP).

To evaluate how the changes in northern hemisphere summer insolation may have influenced the changes in community structure during the deglaciation and Holocene, at Cleland Lake, we compared the June 60°N summer insolation record (Berger and Loutre, 1991) with the pigment-related PCs. Each PC was compared with the Northern hemisphere summer insolation data over the duration of the record after interpolation to a 200-yr time step, consistent with the coarse resolution of summer insolation data. We found significant correlations between two of the components (Fig. 9). Algal and cyanophyte abundances reconstructed by PC 4 and PC 2 significantly correlate with the northern hemisphere summer insolation trend. PC 4 shows a negative correlation ($r = -0.7$, $n = 73$, $p < 0.05$), with summer insolation throughout the

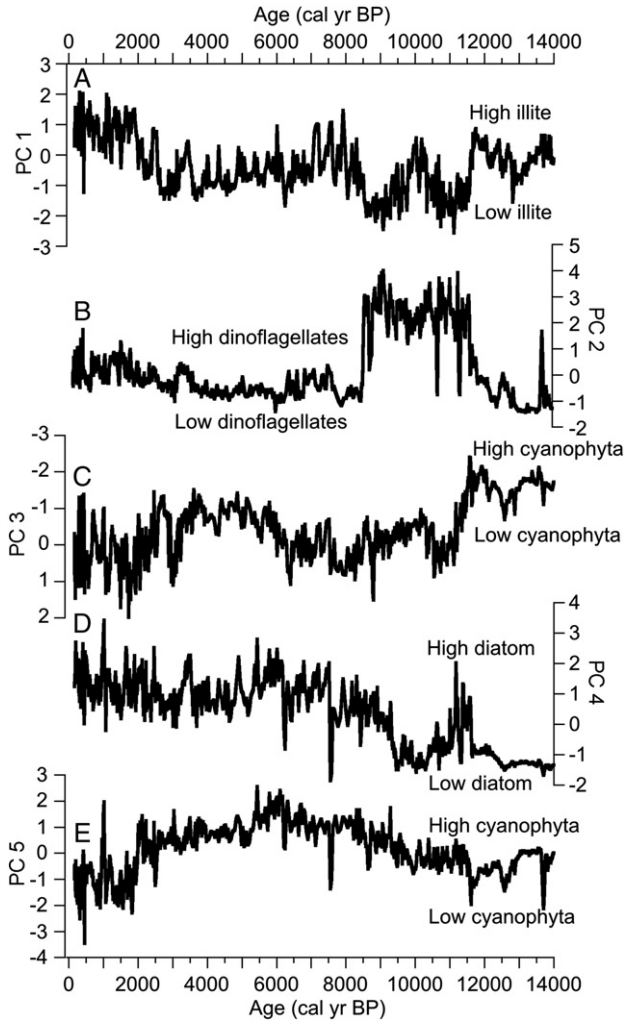

Figure 8. Down-core variation of the first five principal components of the reflectance data, A. principal component 1 clay mineral/runoff proxy, B. principal component 2: dinoflagellate algae abundance proxy, C. principal component 3: cyanophyte abundance proxy, D. principal component 4: diatom and cyanophyte abundance. Note that the y axis in C and D is reversed for the cyanophytes in panel, E. principal component 5: cyanophyte abundance proxy.

record (13,600 cal yr BP to present), indicating low abundance of diatom, but high abundance of cyanophytes in cyanophyte community 2 at lower summer insolation values (Fig. 9). PC 2 has a negative correlation ($r = -0.6$, $n = 43$, $p < 0.05$) to summer insolation during the middle and late Holocene (8600 cal yr BP to present), but above a threshold value of 516 W m^{-2}, which occurs from 13,600 to 8400 cal yr BP, there is a near step-function increase in PC2 abundance, indicating a non-linear response of dinoflagellate abundance to summer insolation (Fig. 9).

Discussion

Interpretation of the principal components

Several factors promote pigment preservation in sediment. Increasing lake depth increases stratification, promotes hypoxia or anoxia and inhibits re-suspension of sediment, thereby promoting pigment preservation (Sanger, 1988). In addition, low light conditions and high sedimentation rates promote the preservation of pigments by reducing photochemical decomposition (Sanger, 1988). Alkaline waters tend to preserve pigments as opposed to acidic waters, which degrade chlorophylls (Sanger, 1988). Previous research documents high pigment preservation potential in shallow, productive lakes (Sanger and Gorham, 1972; Sanger and Crowl, 1979; Sanger, 1988). At Cleland Lake, cold (~6°C), alkaline (pH ~9.5), and anoxic water conditions occur below 5 m depth (Fig. 2). Such conditions enhance the preservation of pigments at all three core sites. The presence of laminated sediment throughout the record (with the exception of between ~10,000 and 8000 cal yr BP) suggests minimal sediment resuspension and improved pigment preservation. It is possible that past variability in pigment preservation affected sediment composition, particularly from 11,000 to 8500 cal yr BP when fewer laminae formed. However, we observe maxima in dinoflagellate- and cyanophyte-related pigments at that time. While our estimates may provide a lower limit on the actual production, if pigment preservation had been reduced during this period, our estimates would likely not suggest an increase in the abundance of dinoflagellate and cyanophytes at that time. We infer that there was little or no difference in pigment preservation at the different core sites and that preservation rates did not vary substantially through time because there is no evidence to support rapid changes in differential preservation.

PC 1, which relates to illite is the only PC that is dominated solely by inorganic material and can be used as a proxy for fluvial input to the lake. Illite, which is present throughout the record, represents detrital clay transported to the lake from the heavily, glacial-drift covered watershed. All of the four remaining components are primarily related to pigment variations in the lake. With respect to PC2, the major photosynthetic pigments of flagellated algae belonging to the division Pyrrophyta includes: chlorophyll-a, chlorophyll-c, and peridinin (Sze, 1993). The

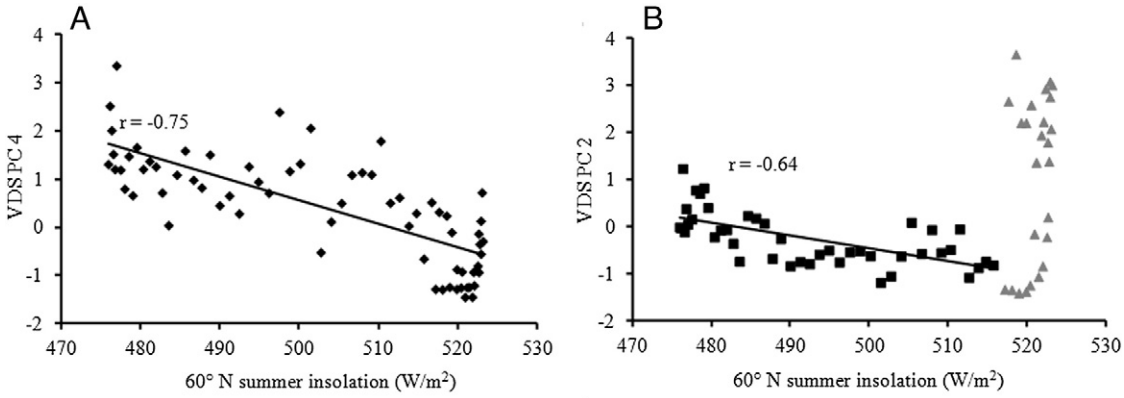

Figure 9. Scatter plots of summer insolation verses the reflectance PC 4 (A) and PC 2 (B). In panel A the black diamonds show the strong linear correlation between PC 4 and summer insolation throughout the record (200–13,600 cal yr BP). In panel B the black squares at 8400–200 cal yr BP and the black line represent the strong linear trend between 8400 and 200 cal yr BP and gray triangles show the non-linear relationship between PC 2 and summer insolation between 8400 and 13,600 cal yr BP.

presence of peridinin and pheophytin-a (a degredation product of chlorophyll-a) in PC 2 identifies this component as a proxy for dinoflagellate abundance in the lake (Sze, 1993). Dinoflagellate algae are common in oligotrophic, high-latitude/polar lakes, or in water with low light intensities, such as snow-covered or turbid lakes (Sze, 1993). Large, positive PC 2 values indicate greater dinoflagellate abundance and low nutrient conditions, or low light intensity. The time series for PC 2 and PC 4 in the three sediment cores from the shallow, intermediate, and deep parts of the lake are used to interpret variability of these PCs within the sediment record and to support the interpretation of PC 2 and PC 4 as paleo-lake level proxies, which we focus on hereafter. PCs 3, 4, and 5 contain variable amounts of cyanophyte algal pigments and hence may represent the succession of three different cyanophyte communities in Cleland Lake. Smectite and chlorite, which are present largely near the base of the core reflect the breakdown of volcanic ash and climate-related, clay minerals transported into the basin during the deglaciation of the Cordilleran Ice Sheet (Rhoton et al., 1979). Climate is one factor among many, however, that governs the formation and deposition of clay minerals in lake basins (e.g. parent material, sedimentary facies, and diagenetic alterations), such that interpretations of clay concentration data should be supported by other proxies (Folkoff and Meentemyer 1987; Ruffell et al., 2002; Liu et al., 2007). PC 4 represents the contrasting appearances of diatoms versus cyanophyte in cyanophyte community 2 in Cleland Lake sediment. Comparison of the PC 4 down-core record with the XRF-derived Si:Ti ratio supports the VDS interpretation. The Si:Ti ratio was low between 10,300 and 9500 cal yr BP, simultaneous with the period of reduced diatom abundance as inferred from PC 4. The transitions between low and high diatom periods inferred from the Si:Ti ratio are generally synchronous with the diatom abundance derived from PC 4. However, the two records are not perfectly matched because post-depositional processes may affect pigment and silica preservation and PC 4 is a mixture of 70% diatom pigment and 30% cyanophyte pigments. PC 5 correlates with cyanophyte accessory pigments. Therefore, this component is considered a proxy for a third cyanophyte assemblage.

Algal and cyanophyte abundances reconstructed by PC 2 and PC 4 significantly correlate with the Northern hemisphere summer insolation trend. Both components exhibit a significant, inverse relationship between summer insolation and abundance, but for PC 4, this relationship only holds below the critical threshold value of 516 Wm^{-2}. Increasing summer insolation results in lower abundance, perhaps by increasing stratification and thus decreasing nutrient supply, or perhaps by decreasing precipitation, which would limit the influx of nutrients to the lake through enhanced aridity. Above the threshold value, the system exhibits a shift in community structure, which results in a rapid, non-linear increase in PC 2 abundance as the system shifts into a new steady state (Fig. 9).

Paleohydrological conditions inferred from phytoplankton abundance

Water level changes in temperate lakes influence light penetration depth, nutrient flux, and water column stratification, which affects nutrient supply to the epilimnion providing a strong control on a lake's biological productivity (Battarbee, 2000; Heinsalu et al., 2008; Nõges and Nõges, 1999; Nõges et al., 2003). At lower water levels, in the presence of sufficient light, nutrient limitation controls phytoplankton growth (Nõges et al., 2003). Such conditions lead to an increase in species adapted to low nutrient availability such as dinoflagellates (Sze, 1993, section 4.3). Diatoms are also sensitive to changing hydrologic and geochemical conditions, such as shifts in water level, salinity or nutrient concentration (Barker et al., 1994; Heinsalu et al., 2008; Nõges et al., 2003). Total diatom abundance, which increases exponentially in deeper lakes (Barker et al., 1994), is a common proxy used to reconstruct lake water depth (Barker et al., 1994; Brugam et al., 1998; Gavin et al., 2011). Increases in lake level are associated with higher diatom abundance in sediment (Barker et al., 1994; Heinsalu et al., 2008). Variations in diatom species composition, as well as the ratio between the littoral/planktonic species, indicate water level changes that can shift littoral sedimentary environments away from or toward the center of the basin (Barker et al., 1994; Brugam et al., 1998; Gavin et al., 2011). However, because the VDS approach only identifies the total diatom (bacillariophycea) pigment concentration, separation between benthic and planktonic species is not possible.

In addition to water level, temperature, and nutrient cycling also play a major role in controlling phytoplankton composition (Nõges et al., 2003; Grover and Chrzanowski, 2006, and references therein). Cyanophytes predominate during the summer months and in warm climates due to their higher temperature tolerance. In contrast, diatoms are more prevalent in cold water (Nõges et al., 2003). Diatom abundance is also influenced by the availability of nutrients. In dimictic lakes, higher temperatures can lead to lake-water stratification, producing nutrient depletion in the epilimnion (Barker et al., 1994; Kalff, 2003). Lakes in temperate regions like southern British Columbia tend to be stratified in the summer and often overturn and mix twice a year, resulting in the resuspension of nutrients and diatom blooms during spring and fall. When the availability of nutrients becomes limiting, diatoms can be replaced by taxa such as green algae or cyanophytes (Grover and Chrzanowski, 2006; Nõges et al., 2003; Sze, 1993 and references therein).

There are several other factors, however, like hydrology, herbivore biomass, turbidity, and light that can also affect phytoplankton abundance (Fabbro and Duivenvoorden, 2000; Flores and Barone, 1998; Kruk et al., 2002). This diversity of controlling mechanisms not only highlights the complexities of using biological proxies to measure climate, but also shows how the biological conditions of the lake are intricately linked to many aspects of the ecosystem and climate. Despite the many potential responses of phytoplankton and cyanophytes to environmental changes, we can use photosynthetic pigments to infer the paleo-environmental conditions at Cleland Lake by partitioning the algal response into independent assemblages (which respond distinctly to the environment), supporting our interpretation using multiple proxies and with cores from different water depths in the basin. In summary, PC 2 from core F-09 can be used as a proxy for lake depth, where higher PC 2 values indicate greater dinoflagellate abundance and a shallower lake, and conversely low PC 2 values indicate decreased dinoflagellate abundance and a relatively deeper lake. PC 4 can be used as a temperature and nutrient proxy. Higher PC 4 values indicate a deeper lake and/or cold, nutrient-rich conditions, with greater diatom abundance and less cyanophytes. Low PC 4 values indicate a lower diatom and greater cyanophyte abundance typical of a nutrient-depleted, stratified lake.

Vertical and horizontal heterogeneity in the spatial distribution of phytoplankton in lakes has been studied since the mid-20th century (Baldi, 1941; George and Heaney, 1978; Heaney and Talling, 1980; Wu et al., 2010). Several investigations support the idea of pronounced horizontal variability of phytoplankton abundance associated with wind-induced water movement (George and Heaney, 1978; Heaney and Talling, 1980; Wu et al., 2010). Considerable variation of phytoplankton amounts in the presence of buoyant cyanophytes and the dinoflagellate algae *Ceratium* was reported from Esthwaite Lake in the Lake District of England (George and Heaney, 1978; Heaney and Talling, 1980), indicating that freshwater algae can develop vertical and horizontal zonation even within small lake environments. A scatter plot of PC 2 vs. PC 4 from cores B-09 (deep water), F-09 (intermediate), and E-09 (shallow) demonstrates that PC scores vary with lake depth (Fig. 10, Table 3). Sediment from the shallow water core contains high concentrations of dinoflagellate- and cyanophyte-related pigments and low concentrations of diatom-related pigments; while the deep-water sediment core indicates a similar cyanophyte and diatom abundance, but lower dinoflagellate pigment concentrations. The intermediate core (F-09) contains a lesser amount of dinoflagellate pigment than the shallow water core, but greater amounts of dinoflagellate pigment

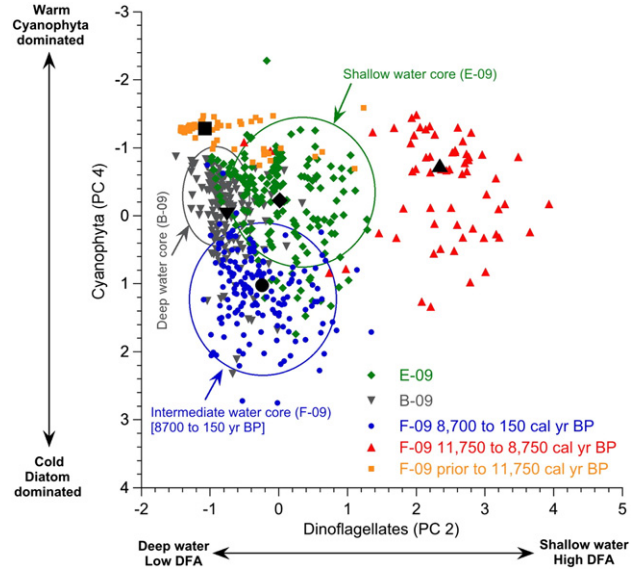

Figure 10. Scatter plot of dinoflagellate algae (DFA, PC 2) versus diatoms and cyanophyte (PC 4) for cores B-09, E-09 and F-09. Fields of color-coded points are enclosed in circles corresponding to water depth. Green diamonds: core E-09 shallow water (7 m); gray triangles: core B-09 deep water (25 m); blue dots: core F-09 intermediate water depth (12.8 m) from 8750 to 150 cal yr BP. Red triangles or orange squares: core F-09 intermediate water depth (12.8 m) from 8750 to 11,750 cal yr BP, or 11,750 to 14,300 cal yr BP, respectively. The large symbol in each cluster depicts the mean PC 2 and PC 4 values for each of the core/water depth and time intervals.

than the deep-water core. The distribution of PC 2 and PC 4 in core F-09 corresponds with the trends at the other two core sites from 8800 to 170 cal yr BP. However, prior to 8800 cal yr BP, diatom and cyanophyte values deviate from the general trend observed in the other cores likely due to lower lake levels during the early Holocene (Figs. 8 and 10). Between 11,600 and 8600 cal yr BP, cyanophyte and dinoflagellate values are high while diatom values are low. Conversely, prior to 11,600 cal yr BP, diatom and dinoflagellate abundances are low, but cyanophyte abundances are high. Comparisons of PC 2 and PC 4 from the three cores at different water depths suggest that PC 2 (dinoflagellate abundance) at core site F-09 is influenced by lake depth, reflecting changes from shallow to deep water facies when the dinoflagellate abundances increase. PC 4 (diatom and cyanophyte abundances) does not show such a clear connection with lake depth. For example, although core B-09 (i.e. the deep water site) has higher diatom abundance than the shallow core (E-09), it contains fewer diatoms than the intermediate water core (F-09), complicating the use of PC 4 as a lake-level proxy. This may be due to the absence of benthic diatom species in the deep-water sediment or minor redox-related preservation differences as a result of physiochemical disparities between the different core sites.

The triangular distribution and spread of the data points in the cross plot between PC 2 and PC 4 for core F-09 indicate that the abundance of the three primary producers is affected by several factors, including temperature and nutrient availability (Nõges et al., 2003 and references therein: Grover and Chrzanowski, 2006). Nonetheless, the scatter plot of PC 2 and PC 4 demonstrates that water depth is an important factor that affects pigment/phytoplankton abundance in PC 2 (Fig. 10).

Temporal pattern of hydroclimatic change

The reflectance-based reconstruction of Cleland Lake productivity shows three distinct periods from the deglaciation through the transition into the Holocene. The first stage can be characterized as a period of low productivity that occurred during the deglaciation from ~14,000 to ~11,800 cal yr BP. Low abundances of diatoms and dinoflagellates and higher amounts of cyanophytes are recorded during this period. Increased runoff from glacial melt water might have contributed to higher lake levels at this time. A higher percentage of mineral matter in the LOI data and higher illite input (suggested by PC 1) supports the idea of greater runoff-related clastic input to the lake from the local watershed (Figs. 8 and 11). During this period, the lake was young, with limited productivity, and we infer in its early successional stages. During the second period (between 11,600 and 8600 cal yr BP), cyanophyte and dinoflagellate abundances peaked, likely in response to the maxima in summer solar insolation. Lesser precipitation amounts and higher temperatures at this time likely limited nutrient input and produced lower lake levels, which favored the growth of cyanophytes over diatoms. Higher temperatures led to stratified lake conditions, possibly leading to further nutrient depletion and thereby reducing diatom abundance. Reduced runoff to the lake is also suggested by a rapid drop in illite concentration between 11,750 and 11,150 cal yr BP. Illite levels remain low between 11,100 and 8600 cal yr BP, simultaneous with the dry period.

The third productivity period started around 8500 cal yr BP with a rapid drop in dinoflagellate levels. This suggests a transition to greater precipitation amounts and an increase in nutrient fluxes, which produced higher diatom concentrations and an increase in lake-level. The synchronous increase in illite (8500 ± 200 cal yr BP) further supported an increase in runoff to the lake (Fig. 8). After this rapid transition from a warm, dry early Holocene to a wet middle to late Holocene, several decadal- to century-scale changes occurred around 7500, 6400, 3250, 2450, 1550, and 800 cal yr BP. Moreover, the transition from the deglaciation to early Holocene low stand, followed by the shift back to higher water levels, implies that large P/E transitions likely occurred over the span of several centuries (or perhaps less time) (e.g. 11,850 to 11,600 and from 8600 to 8500 cal yr BP).

The presence of an early Holocene dry period is also supported by sedimentological analysis of the intermediate core. The stratigraphy transitions from being poorly laminated to massive and carbonate-rich between 11,500 and 8700 and cal yr BP. Corresponding with these depths, LOI-derived calcium carbonate percentage and XRF-derived Ca concentrations rapidly rise between 12,800 and 11,400 (from 16% to 40% and 16,100 to 117,100 cps) and remain high until 8700 cal yr BP (Fig. 5). This sedimentological evidence supports a low stand between 11,500 and 8700 cal yr BP. Finely laminated, organic-rich sediment, and higher organic matter percentages at the top of the core (between 200 and 8100 cal yr BP) indicate the occurrence of a high stand during the middle and late Holocene.

Table 3
Average values of PC 2 and PC 4 for three sediment cores from Cleland Lake.

Core	Water depth (m)	170 to 8800 cal yr BP		8800 to 11,800 cal yr BP		11,800 to 14,000 (prior to 12,000) cal yr BP	
		PC 2	PC 4	PC 2	PC 4	PC 2	PC 4
B-09	20.2 deep	−0.79	0.014				
F-09	12.8 intermediate	−0.27	1.14	2.32	−0.43	−0.77	−0.16
E-09	7 shallow	0.29	−0.43				

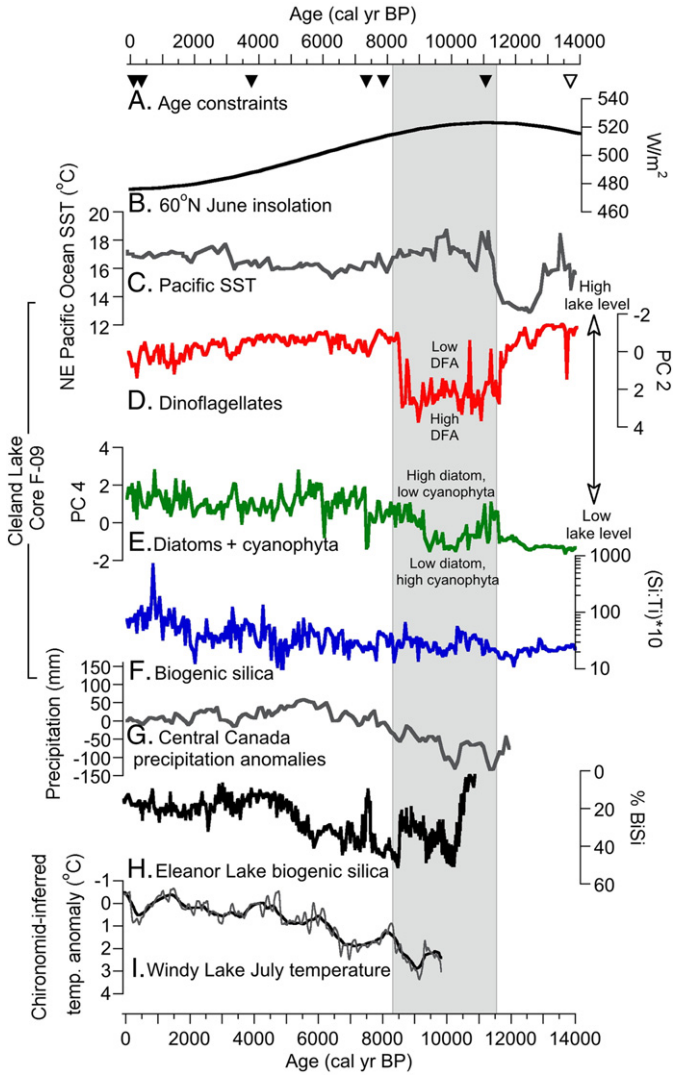

Figure 11. Down-core variation of PC 2, PC 4 and Si:Ti ratios from core F-09 compared with summer insolation at 60°N, sea surface temperature (SST) of Northeastern Pacific Ocean and three independent paleoclimatic reconstructions from southern British Columbia. A. Age model control points of the Cleland lake F-09 core, (filled triangles) ^{14}C and tephra ages, (open triangles) extrapolated age. B. Northern hemisphere June incoming solar radiation at 60°N (Berger and Loutre, 1991). C. Alkenone based SST from ODP Site 1019 in the California margin (41°40′.8 N, 124°55′.8 W) (Barron et al., 2003), D. Dinoflagellate algae abundance derived from diffuse spectral reflectance PC 2. E. Diatom and cyanophyte abundances derived from diffuse spectral reflectance PC 4. F. Si:Ti ratios for core F-09. Note that the y-axis of Si:Ti plot is represented on a log scale to enhance the visualization of the data. Periods of the highest dinoflagellate and cyanophyte abundance are consistent with the peak summer insolation (gray shaded box). G. Annual precipitation anomaly from central boreal Canada (50–70°N, 80–120°W, Viau et al., 2002). H. Percent biogenic silica record from Eleanor Lake (Gavin et al., 2011). I. Combined chironomid-inferred summer temperature anomalies from four sites; Frozen Lake (Rosenberg et al., 2004), North Crater Lake and Lake-of-the-Woods (Palmer et al., 2002), and Windy Lake (Chase et al., 2008) (after Gavin et al., 2011).

Regional comparison during the deglaciation and early Holocene

Additional support for the reflectance-based, paleohydrological and paleoproductivity reconstruction at Cleland Lake can be found in the existing paleoclimate literature from British Columbia. During the late glacial and early Holocene, rapid and significant vegetational and climatic fluctuations occurred in southern British Columbia (Pellatt et al., 2002). Deglaciation, alpine glacial advances, Younger Dryas cooling and rapid early Holocene temperature changes occurred over this period (Pellatt et al., 2002). Palynological and paleo-environmental climatic reconstructions suggest the Holocene climate of southern British Columbia can be divided into three distinct zones consisting of a cold and dry deglacial period, early Holocene dry period and a cold, wet middle to late Holocene (Alley, 1976; Mathews and Heusser, 1981; Pellatt et al., 2002; Walker and Pellatt, 2003; Hallett and Hills, 2006; Galloway et al., 2011; Gavin et al., 2011). In Cleland Lake sediment, the same Holocene climatic pattern is expressed as variations in pigment concentrations, which occurred at similar times.

Fossil midge-based temperature reconstructions and several pollen analyses from locations around Cleland Lake suggest that the deglacial period in southern British Columbia was −1 to −2°C colder than present (Matthews and Heusser, 1981; Chase et al., 2008). The cold, moist, deglacial climate between 12,000 and 10,500 ^{14}C yr BP (Mathews and Heusser, 1981), when calibrated using CLAM 1.0.2 yields ages of 14,000 and 12,150 cal yr BP was followed by a rapid decrease in precipitation and increase in temperature from 10,500 to 10,000 ^{14}C yr BP (calibrated ages 12,150 to 11,500 cal yr BP; Alley, 1976; Mathews and Heusser, 1981; Chase et al., 2008). This timing is synchronous with the rapid onset of drier conditions at Cleland Lake (11,700 ± 100 cal yr BP).

Several modeling and pollen-based temperature and precipitation reconstructions throughout southern British Columbia suggest that relative to present, early Holocene summer temperatures were +5 to +10°C warmer and precipitation was about 30% lower, (Mathews and 1981; Bartlein et al., 1998; Chase et al., 2008). This is consistent with the low stand we infer from pigments at Cleland Lake during the early Holocene. The rapid transition to a warm early Holocene is also suggested by midge-based reconstructions from southeastern British Columbia (Palmer et al., 2002; Rosenberg et al., 2004; Chase et al., 2008, Figs. 1 and 11). Other studies indicate that summer temperatures from 10,500 to 9000 cal yr BP were likely +3 to +4°C warmer than present (Chase et al., 2008). At Big Lake, 30 km east of Cleland Lake, a lake level reconstruction based on *Charophyte* accumulation rates indicates lower water level from 10,300 to 8500 cal yr BP (Hallett and Hills, 2006). Sediment dating to 10,200 cal yr BP from Eleanor Lake, located 250-km northwest of Cleland Lake, contain high concentrations of biogenic silica, indicating more open water on this lake during early Holocene (9300–8500 cal yr BP) contrasting with other regional records (Gavin et al., 2011, Fig. 11).

Pollen-based, regional climatic reconstructions from Canada reveal a warm, dry early Holocene (between 12,000 and 10,000 cal yr BP) in the central Canadian region (50–70°N, 80–120°W, Viau et al., 2002, Fig. 11). In addition, elevated percentages of xerohpyte plant taxa from the same location (*Pinus juniperus*, *Artemmisia*, *Poaceae*) provide evidence that a drier climate existed prior to 8500 cal yr BP (Hallett and Hills, 2006). A much longer warm interval between 10,000 to 4900 cal yr BP was recorded in sediment from Mahoney Lake; located in the semi-arid Okanagan valley southwest of Cleland Lake (Lowe et al., 1997). The presence of tree stumps at elevations higher than the present tree line in British Columbia, further suggests that temperatures were warmer at this time (Chase et al., 2008 and references therein). In general, these studies and others (e.g. Matthews and Heusser, 1981) indicate that the early Holocene was warmer and drier than present, which is supported by the spectral reflectance-based reconstructions at Cleland Lake.

The rapid drop in dinoflagellate values in Cleland Lake around 8600 yr BP suggests a return to cooler, wetter conditions. This observation is supported by the arrival of *Pseudotsuga*/*Larix* pollen to the Kootenay valley (Hallett and Hills, 2006). The sharp decrease in fire frequency around Dog Lake, southern British Columbia (32 km west of Cleland Lake) after 9000 cal yr BP could also be interpreted as an increase in effective moisture, although other factors may have contributed to this change (Hallett and Hills, 2006). Rapid increases in summer moisture and lower temperatures between 9300 and 8500 cal yr BP are also suggested by a reduction of biogenic silica abundances at Eleanor Lake, in response to cooling that would have decreased the length of the summer production season (Gavin et al., 2011, Fig. 8).

This colder, more ice-covered lake experienced a warm dry period between 8500 and 5000 cal yr BP, contrasting with the other regional records (Gavin et al., 2011). At Cleland Lake, this cooler, wet period is concurrent with an increase in diatom abundances as inferred from pigments and Si/Ti ratios because the local micro-climate shifted from an arid one, to a wetter one, associated with increased fluvial input to the lake, greater water depth, and thus a higher nutrient flux, supporting a larger diatom community.

Although paleorecords from the region are largely consistent, some of the differences can be explained by the disparity in lake hydrologic setting, intra-regional climate heterogeneity, and seasonal weighting of different paleoclimate proxies. In general, the timing of the reflectance-based reconstructions from Cleland Lake corresponds with other climate reconstructions from the region.

The prolonged period of heightened dryness in southern British Columbia during the late Pleistocene and early Holocene was likely driven by summer insolation-related amplification of the subtropical, North Pacific, and Bermuda high-pressure systems (Bartlein et al., 1998; Knapp et al., 2004; Renssen et al., 2009). Modeling results from Bartlein et al. (1998) suggest that the surface–air temperature of the interior Pacific Northwest of North America is largely controlled by air temperature in the upper troposphere. Simulations of sea-level pressure suggest that an ~8% increase in northern hemisphere summer insolation as occurred during the middle Holocene Thermal Maximum (HTM) resulted in a strengthening of the eastern Pacific and Bermuda subtropical high-pressure systems (Bartlein et al., 1998). The development of such a blocking pressure system would have reduced the transport of moist westerly air into the interior regions of the Pacific Northwest of North America (Stahl et al., 2006). The spatial and temporal expression of this period of dryness was likely highly variable due to the large geographic disparities (i.e. elevation, topography, climate), which determine the numerous micro-climates across the interior Pacific Northwest (Diffenbaugh and Sloan, 2004; Diffenbaugh et al., 2006; Shin et al., 2006; Shinker and Bartlein, 2010). We propose that summer insolation-driven changes in air temperature moderated moisture delivery to Cleland Lake by altering the configuration of the subtropical high-pressure systems (Bartlein et al., 1998).

Reorganization of the climate system associated with the collapse of the Laurentide ice sheet (LIS) between 10,000 and 8000 cal yr BP triggered rapid changes in the climate of North America (Shuman et al., 2002; Renssen et al., 2009; Williams et al., 2010). Various paleoclimate proxies from the middle and high-latitudes of the Northern Hemisphere record a relatively warm climate during the HTM (Viau et al., 2002; Renssen et al., 2009). The timing and the magnitude of this event varied substantially between regions (Kaufman et al., 2004; Renssen et al., 2009 and references therein). For example, in Alaska and northwestern Canada the HTM occurred from 11,000 to 9000 cal yr BP; in north central Canada the warming occurred between 8000 and 5000 cal yr BP (Kaufman et al., 2004 and references therein); while in Northwestern America it occurred between 8000 and 5000 cal yr BP (Stone and Fritz, 2006; Whitlock et al., 2012). Lake-level and pollen data from northwestern America show conditions drier than modern coastal conditions between 11,000 and 8200 cal yr BP (Whitlock et al., 2012). In contrast, a transition to wet conditions is recorded by lake level and pollen records from the southeastern United States (Shuman et al., 2002, 2009, 2010). In the north-central United States, wet conditions are recorded 10,000 cal yr BP and a transition to a drier climate occurs from 9000 to 8000 cal yr BP (Shuman et al., 2002). The strengthening of the Bermuda subtropical high-pressure system and the deflection of moisture sources from the Gulf of Mexico associated with the deterioration of the LIS led to the development of these dry conditions (Shuman et al., 2002; Williams et al., 2010). However, modeling studies suggest that the LIS does not have as direct impact on the HTM in western Canada (see figure 2 in Renssen et al., 2009), perhaps in part because this region lies on the western side of the mountains relative to the changes driven by the LIS collapse to the east. The HTM in western Canada occurred simultaneous with the Holocene summer insolation maximum of the Northern Hemisphere; whereas the delayed warming in central and eastern Canada likely resulted from atmospheric and ocean circulation changes associated with the collapsing LIS (Fig. 2, Renssen et al., 2009).

The sediment core data from Cleland Lake suggest a pattern of climate change in southeastern British Columbia during the Pleistocene–Holocene transition similar to that of other paleoclimate records from the region. Alkenone-derived SST suggest relatively warm northeastern Pacific Ocean conditions during the early Holocene (11,600–8200 cal yr BP) (Barron et al., 2003, Fig. 11). Pacific Ocean SST changes are strongly coupled to that of North Atlantic Ocean (Peteet et al., 1997; Kienast and McKay 2001; Barron et al., 2003). The late Pleistocene–early Holocene opening of the Bering Strait allowed the passage of relatively fresh Pacific water into the Atlantic Ocean, leading to global-scale changes to the meridional redistribution of heat and fresh water (Peteet et al., 1997; Kienast and McKay 2001; Ortiz et al., 2009; Hu et al., 2010; Ortiz et al., 2012). Numerical modeling studies show that the closing of Bering Strait gives rise to positive temperature anomalies in Europe and North Africa, and negative temperature anomalies in Northwestern America (Hu et al., 2010). Hence rapid and abrupt early Holocene warming recorded across North America could be linked to this Pacific to Atlantic teleconnection (Peteet et al., 1997; Kienast and McKay 2001). The abrupt changes (possibly over several centuries or less) that marked the beginning and end of the HTM are likely the result of a summer insolation-driven, non-linear response (as the climate system passes through a threshold) resulting from a positive feedback between vegetation and the land surface, ocean, and atmosphere. Similar non-linear responses were reported from Western Sahara and Eastern Africa, during the initiation and the termination of the African humid period (DeMenocal et al., 2000; Tierney et al., 2008; Tierney and deMenocal, 2013). The teleconnection linking the tropics and Southwestern Canada is likely the atmospheric blocking pattern associated with the eastern Pacific and Bermuda subtropical high-pressure system and the modifications to Atlantic Meridional Overturning Circulation with the opening of the Bering Strait.

Climate models simulating atmospheric conditions have demonstrated that a 40% increase in North African rainfall can result from an 8% increase in summer radiation (DeMenocal et al., 2000). Paleoclimate data from western North America as well as other parts of the world provide evidence of prolonged droughts in the early–middle Holocene that lasted for centuries to millennia (e.g., Overpeck and Cole, 2006). These prolonged, severe droughts resulted from non-linear responses of the climate system to radiative forcing (Viau et al., 2002; Overpeck and Cole, 2006; Clegg et al., 2011) and therefore hint at the possibility that an analogous climate change could occur in the future in response to anthropogenic, greenhouse gas forcing, although rising sea level will negate the role that an opening Bering Strait played during the HTM. The combined effect of a warming ocean and a positive feedback from reduced soil moisture in an anthropogenically warming world could enhance the probability of prolonged droughts (Overpeck and Cole, 2006), although the details of the response likely will depend on the interaction of greenhouse forcing and summer solar insolation.

Conclusions

Cleland Lake is a small, alkaline, closed-basin lake that is hydrologically and geochemically sensitive to drought. Phytoplankton communities are influenced by lake responses to hydroclimate variability. We employed visible derivative spectroscopy to measure ancient phytoplankton pigments in Cleland Lake sediment cores to infer algal abundance and distribution and to thereby reconstruct lake productivity and hydrologic balance throughout the latest Pleistocene and Holocene. Our analysis suggests that lake productivity was low and mostly limited to early successional, cyanophyte communities during the late Pleistocene deglaciation (prior to 11,600 cal yr BP). Dinoflagellates rapidly increased

after 11,800 and remained high between 11,600 and 8600 cal yr BP, indicating warm, low lake-level conditions. Low diatom and high cyanophyte concentrations between 11,500 and 9500 cal yr BP further indicate a warm, shallow lake at this time. The magnitude of early Holocene lake-level change was likely greater than that of the middle and late-Holocene. Dinoflagellate-related algal pigments decrease rapidly after 8500 cal yr BP, suggesting a transition to wet conditions and higher lake levels. This interpretation is further strengthened by illite input to the lake as represented by PC 1, sedimentological evidence from the comparison of PCs between cores from different water depths, as well as comparison with other paleoclimate records from the region, which show similar patterns.

Lake-level changes inferred from variations in the concentration of dinoflagellate algae and cyanophytes in Cleland Lake sediment cores indicate that lower lake levels were coincident with the Northern Hemisphere summer insolation maximum, which occurred between ~11,500 and 8700 cal year BP at this latitude. Lake levels increased after 8500 cal yr BP and remained relatively higher until present, implying wetter conditions more consistent with the modern climate of the region. The abrupt shift to low lake levels and relatively dry conditions that characterized the late Pleistocene–Holocene transition (and the corresponding rapid return to wetter conditions thereafter) were likely driven by non-linear climate responses to orbital forcing and a resulting amplification of the subtropical, North Pacific high-pressure system, which reduced moist, westerly air flow from the Pacific Basin to Cleland Lake.

Supplementary data to this article can be found online at http://dx.doi.org/10.1016/j.yqres.2015.02.003.

Acknowledgments

This research was supported by funding from National Science Foundation to the University of Pittsburgh, (EAR-0902200) and Kent State University (EAR-0902753). BAS acknowledges the NSF Atmospheric and Geospace Sciences Postdoctoral Research Program (AGS 1137750). DPP acknowledges the Andrew W. Mellon Predoctoral Fellowship at the University of Pittsburgh.

References

Abbott, M.B., Stafford Jr., T.W., 1996. Radiocarbon geochemistry of modern and ancient arctic lake systems, Baffin island, Canada. Quaternary Research 45 (3), 300–311.
Alley, N., 1976. The palynology and palaeoclimatic significance of a dated core of Holocene peat, Okanagan valley, southern British Columbia. Canadian Journal of Earth Sciences 13 (8), 1131–1144.
Alley, R.B., Marotzke, J., Nordhaus, W., Overpeck, J., Peteet, D., Pielke, R., Pierrehumbert, R., Rhines, P., Stocker, T., Talley, L., 2003. Abrupt climate change. Science 299, 2005–2010.
Baldi, E., 1941. Mechanismus der Rotfarbung im Tovel-See. Archiv fur Hydrobiologie (Mechanism of red coloration in Tovel-See). (Freshwater Biological Association translation (New Series), No. 97. Available from the Librarian, Freshwater Biological Association.). 38 pp. 299–302.
Barker, P., Roberts, N., Lamb, H., Van der Kaars, S., Benkaddour, A., 1994. Interpretation of Holocene lake-level change from diatom assemblages in Lake Sidi Ali, middle atlas, Morocco. Journal of Paleolimnology 12 (3), 223–234.
Barron, J.A., Heusser, L., Herbert, T., Lyle, M., 2003. High-resolution climatic evolution of coastal northern California during the past 16,000 years. Paleoceanography 18 (1), 1020.
Bartlein, P.J., Anderson, K.H., Anderson, P., Edwards, M., Mock, C., Thompson, R.S., Webb, R.S., Webb III, T., Whitlock, C., 1998. Paleoclimate simulations for North America over the past 21,000 years, features of the simulated climate and comparisons with paleoenvironmental data. Quaternary Science Reviews 17 (6–7), 549–585.
Battarbee, R.W., 2000. Palaeolimnological approaches to climate change, with special regard to the biological record. Quaternary Science Reviews 19 (1), 107–124.
Berger, A., Loutre, M., 1991. Insolation values for the climate of the last 10 million years. Quaternary Science Reviews 10 (4), 297–317.
Blaauw, M., 2010. Methods and code for classical age-modeling of radiocarbon sequences. Quaternary Geochronology 5, 512–518.
Bouchard, F., Pienitz, R., Ortiz, J.D., Francus, P., Laurion, I., 2013. Palaeolimnological conditions inferred from fossil diatom assemblages and derivative spectral properties of sediments in thermokarst ponds of subarctic Quebec, Canada. Boreas 42 (3), 575–595.
Brenner A.R., 2014. Determination of Baffin Bay sediment composition variability and provenance, unpublished master thesis, pp 99.
Brown, E.T., 2011. Lake Malawi's response to "megadrought" terminations: sedimentary records of flooding, weathering and erosion. Palaeogeography, Palaeoclimatology, Palaeoecology 303 (1–4), 120–125.
Brown, E.T., Johnson, T., Scholz, C., Cohen, A., King, J., 2007. Abrupt change in tropical African climate linked to the bipolar seesaw over the past 55,000 years. Geophysical Research Letters 34 (20), L20702.
Brugam, R.B., McKeever, K., Kolesa, L., 1998. A diatom-inferred water depth reconstruction for an upper peninsula, Michigan Lake. Journal of Paleolimnology 20 (3), 267–276.
Chase, M., Bleskie, C., Walker, I.R., Gavin, D.G., Hu, F.S., 2008. Midge-inferred holocene summer temperatures in southeastern British Columbia, Canada. Palaeogeography, Palaeoclimatology, Palaeoecology 257 (1), 244–259.
Clark, R.N., Swayze, G.A., Wise, R., Livo, E., Hoefen, T., Kokaly, R., Sutley, S.J., 2007. USGS Digital Spectral Library splib06a: U.S. Geological Survey, Digital Data Series 231.
Clegg, B.F., Kelly, R., Clarke, G.H., Walker, I.R., Hu, F.S., 2011. Nonlinear response of summer temperature to Holocene insolation forcing in Alaska. Proceedings of the National Academy of Sciences 108 (48), 19299–19304.
Connell, J.H., Slatyer, R.O., 1977. Mechanisms of succession in natural communities and their role in community stability and organization. American Naturalist 111 (982), 1119–1144.
Cook, E.R., Woodhouse, C.A., Eakin, C.M., Meko, D.M., Stahle, D.W., 2004. Long-term aridity changes in the western United States. Science 306 (5698), 1015–1018.
Cook, E.R., Seager, R., Heim, R.R.J., Vose, R.S., Herweijer, C., Woodhouse, C., 2010. Megadroughts in North America: placing IPCC projections of hydroclimatic change in a long-term palaeoclimate context. Journal of Quaternary Sciences 25, 48–61.
Das, B., Vinebrooke, R.D., Sanchez-Azofeifa, A., Rivard, B., Wolfe, A.P., 2005. Inferring sedimentary chlorophyll concentrations with reflectance spectroscopy: a novel approach to reconstructing historical changes in the trophic status of mountain lakes. Canadian Journal of Fisheries and Aquatic Sciences 62 (5), 1067–1078.
deMenocal, P., Ortiz, J., Guilderson, T., Adkins, J., Sarnthein, M., Baker, L., Yarusinsky, M., 2000. Abrupt onset and termination of the African humid period: rapid climate responses to gradual insolation forcing. Quaternary Science Reviews 19 (1), 347–361.
Diffenbaugh, N.S., Sloan, L.C., 2004. Mid-Holocene orbital forcing of regional-scale climate: a case study of Western North America using a high-resolution RCM. Journal of Climate 17 (15), 2927–2937.
Diffenbaugh, N.S., Ashfaq, M., Shuman, B., Williams, J.W., Bartlein, P.J., 2006. Summer aridity in the United States: response to mid-Holocene changes in insolation and sea surface temperature. Geophysical Research Letters 33, L22712.
Eberl, D.D., 2003. User guide to RockJock—a program for determining quantitative mineralogy from X-ray diffraction data. USGS Open File Report OF 03-78p. 40.
Eberl, D.D., 2004. Quantitative mineralogy of the Yukon River system: variations with reach and season, and determining sediment provenance. American Mineralogist 89, 1784–1794.
Fabbro, L.D., Duivenvoorden, L.J., 2000. A two-part model linking multidimensional environmental gradients and seasonal succession of phytoplankton assemblages. Hydrobiologia 438 (1), 13–24.
Flores, L.N., Barone, R., 1998. Phytoplankton dynamics in two reservoirs with different trophic state (Lake Rosamarina and Lake Arancio, Sicily, Italy). Hydrobiologia 369, 163–178.
Folkoff, M.E., Meentemeyer, V., 1987. Climatic control of the geography of clay minerals genesis. Annals of the Association of American Geographers 77 (4), 635–650.
Fritz, S.C., 2008. Deciphering climatic history from lake sediments. Journal of Paleolimnology 39 (1), 5–16.
Galloway, J.M., Lenny, A.M., Cumming, B.F., 2011. Hydrological change in the central interior of British Columbia, Canada: diatom and pollen evidence of millennial-to-centennial scale change over the Holocene. Journal of Paleolimnology 45 (2), 183–197.
Gantt, E., 1975. Phycobilisomes: light-harvesting pigment complexes. Bioscience 25 (12), 781–788.
Gavin, D.G., Henderson, A.C.G., Westover, K.S., Fritz, S.C., Walker, I.R., Leng, M.J., Hu, F.S., 2011. Abrupt Holocene climate change and potential response to solar forcing in western Canada. Quaternary Science Reviews 30 (9), 1243–1255.
George, D., Heaney, S., 1978. Factors influencing the spatial distribution of phytoplankton in a small productive lake. Journal of Ecology 66 (1), 133–155.
Graham, L., Wilcox, L., 2000. Algae. Prentice Hall, p. 640.
Grover, J.P., Chrzanowski, T.H., 2006. Seasonal dynamics of phytoplankton in two warm temperate reservoirs: association of taxonomic composition with temperature. Journal of Plankton Research 28 (1), 1–17.
Hallett, D.J., Hills, L.V., 2006. Holocene vegetation dynamics, fire history, lake level and climate change in the Kootenay valley, southeastern British Columbia, Canada. Journal of Paleolimnology 35 (2), 351–371.
Heaney, S., Talling, J., 1980. Dynamic aspects of dinoflagellate distribution patterns in a small productive lake. Journal of Ecology 68 (1), 75–94.
Heinsalu, A., Luup, H., Alliksaar, T., Nõges, P., Nõges, T., 2008. Water level changes in a large shallow lake as reflected by the plankton:periphyton-ratio of sedimentary diatoms. European Large Lakes Ecosystem Changes and their Ecological and Socioeconomic Impacts. 599(1) pp. 23–30.
Heiri, O., Lotter, A.F., Lemcke, G., 2001. Loss on ignition as a method for estimating organic and carbonate content in sediments: Reproducibility and comparability of results. Journal of Paleolimnology 25 (1), 101–110.
Hu, A., Meehl, G.A., Otto-Bliesner, B.L., Waelbroeck, C., Han, W., Loutre, M., Lambeck, K., Mitrovica, J.X., Rosenbloom, N., 2010. Influence of Bering strait flow and north Atlantic circulation on glacial sea-level changes. Nature Geoscience 3 (2), 118–121.
Johnson, T.C., Brown, E.T., Shi, J., 2011. Biogenic silica deposition in lake Malawi, east Africa over the past 150,000 years. Palaeogeography, Palaeoclimatology, Palaeoecology 303 (1–4), 103–109.
Kalff, J., 2003. Limnology: inland water ecosystems. Prentice Hall, p. 592.
Kaufman, D., Ager, T., Anderson, N., Anderson, P., Andrews, J., Bartlein, P., et al., 2004. Holocene thermal maximum in the western Arctic (0–180 W). Quaternary Science Reviews 23 (5), 529–560.
Kienast, S.S., McKay, J.L., 2001. Sea surface temperatures in the subarctic northeast Pacific reflect millennial-scale climate oscillations during the last 16 kyrs. Geophysical Research Letters 28 (8), 1563–1566.
Knapp, P.A., Soulé, P.T., Grissino-Mayer, H.D., 2004. Occurrence of sustained droughts in the interior Pacific Northwest (AD 1733–1980) inferred from tree-ring data. Journal of Climate 17, 140–150.
Kruk, C., Mazzeo, N., Lacerot, G., Reynolds, C., 2002. Classification schemes for phytoplankton: a local validation of a functional approach to the analysis of species temporal replacement. Journal of Plankton Research 24 (9), 901–912.
Leng, M.J., Marshall, J.D., 2004. Palaeoclimate interpretation of stable isotope data from lake sediment archives. Quaternary Science Reviews 23 (7–8), 811–831.

Liu, Z., Colin, C., Huang, W., Le, K.P., Tong, S., Chen, Z., et al., 2007. Climatic and tectonic controls on weathering in south China and Indochina Peninsula: clay mineralogical and geochemical investigations from the pearl, red, and Mekong drainage basins. Geochemistry, Geophysics, Geosystems 8 (5), 1–18.
Lowe, D.J., Green, J.D., Northcote, T.G., Hall, K.J., 1997. Holocene fluctuations of a meromictic lake in southern British Columbia. Quaternary Research 48 (1), 100–113.
Mann, M.E., Cane, M.A., Zebiak, S.E., Clement, A., 2005. Volcanic and solar forcing of the tropical Pacific over the past 1,000 years. Journal of Climate 18 (3), 447–456.
Mathewes, R.W., Heusser, L.E., 1981. A 12,000 year palynological record of temperature and precipitation trends in southwestern British Columbia. Canadian Journal of Botany 59 (5), 707–710.
Mayewski, P.A., Rohling, E.E., Curt Stager, J., Karlén, W., Maasch, K.A., David Meeker, L., Meyerson, E.A., Gasse, F., van Kreveld, S., Holmgren, K., Lee-Thorp, J., Rosqvist, G., Rack, F., Staubwasser, M., Schneider, R.R., Steig, E.J., 2004. Holocene climate variability. Quaternary Research 62, 243–255.
McCabe, G.J., Palecki, M.A., Betancourt, J.L., 2004. Pacific and Atlantic Ocean influences on multidecadal drought frequency in the United States. Proceedings of the National Academy of Sciences 101 (12), 4136.
Moore, R., Spittlehouse, D., Whitfield, P., Stahl, K., 2010. Weather and climate. Compendium of Forest Hydrology and Geomorphology in British Columbia (Editors RG Pike, TE Redding, RD Moore, RD Winkler, KD Bladon) Land Management Handbook 66, 47–84.
Müller-Navarra, D., Güss, S., von Storch, H., 1997. Interannual variability of seasonal succession events in a temperate lake and its relation to temperature variability. Global Change Biology 3 (5), 429–438.
Nara, F., Tani, Y., Soma, Y., Soma, M., Naraoka, H., Watanabe, T., et al., 2005. Response of phytoplankton productivity to climate change recorded by sedimentary photosynthetic pigments in lake Hovsgol (Mongolia) for the last 23,000 years. Quaternary International 136 (1), 71–81.
Nelson, D.B., Abbott, M.B., Steinman, B., Polissar, P.J., Stansell, N.D., Ortiz, J.D., Rosenmeier, M.F., Finney, B.P., Riedel, J., 2011. Drought variability in the Pacific northwest from a 6,000-yr lake sediment record. Proceedings of the National Academy of Sciences 108 (10), 3870–3875.
Nõges, T., Nõges, P., 1999. The effect of extreme water level decrease on hydrochemistry and phytoplankton in a shallow eutrophic lake. Hydrobiologia 408 (409), 277–283.
Nõges, T., Nõges, P., Laugaste, R., 2003. Water level as the mediator between climate change and phytoplankton composition in a large shallow temperate lake. Hydrobiologia 506 (1–3), 257–263.
Ortiz, J.D., 2011. Application of Visible/near Infrared derivative spectroscopy to Arctic paleoceanography, IOP Conference. Series: Earth and Environmental Science 14, pp. 1–13.
Ortiz, J.D., Mix, A., Harris, S., O'Connell, S., 1999. Diffuse spectral reflectance as a proxy for percent carbonate content in north Atlantic sediments. Paleoceanography 14 (2), 171–186.
Ortiz, J.D., Polyak, L., Grebmeier, J.M., Darby, D.A., Eberl, D.D., Naidu, S., Nof, D., 2009. Provenance of Holocene sediment on the Chukchi-Alaskan margin based on combined diffuse spectral reflectance and quantitative X-ray diffraction analysis. Global and Planetary Change 68, 73–84.
Ortiz, J.D., Nof, D., Polyak, L., St-Onge, G., Lisé-Pronovost, A., Naidu, S., Darby, D., Brachfeld, S., 2012. The Late Quaternary flow through the Bering Strait has been forced by the Southern Ocean winds. Journal of Physical Oceanography 42 (11), 2014–2029.
Overpeck, J.T., Cole, J.E., 2006. Abrupt change in Earth's climate system. Annual Review of Environment and Resources 31, 1–31.
Palmer, S., Walker, I., Heinrichs, M., Scudder, G., 2002. Postglacial midge community change and Holocene palaeotemperature reconstructions near treeline, southern British Columbia (Canada). Journal of Paleolimnology 28 (4), 469–490.
Peet, R.K., Christensen, N.L., 1980. Succession: a Population Process. Springer, p. 140.
Pellatt, M.G., Mathewes, R.W., Clague, J.J., 2002. Implications of a late-glacial pollen record for the glacial and climatic history of the Fraser lowland, British Columbia. Palaeogeography, Palaeoclimatology, Palaeoecology 180 (1), 147–157.
Peteet, D., Beck, W., Ortiz, J., O'Connell, S., Kurdyla, D., Mann, D., 2003. Rapid vegetational and sediment change from Rano Aroi Crater, Easter Island. In: Loret, J., Tanacredi, J. (Eds.), Easter Island: Scientific Exploration into the World's Environmental Problems in Microcosm. Kluwer/Plenum Publishers, pp. 81–92.
Peteet, D., Del Genio, A., Lo, K.K.W., 1997. Sensitivity of northern hemisphere air temperatures and snow expansion to North Pacific sea surface temperatures in the Goddard Institute for Space Studies general circulation model. Journal of Geophysical Research: Atmospheres (1984–2012) 102 (D20), 23781–23791.
Pickett, S., Collins, S., Armesto, J., 1987. Models, mechanisms and pathways of succession. The Botanical Review 53 (3), 335–371.
Pompeani, D., Steinman, B., Abbott, M., 2012. A sedimentary and geochemical record of water-level changes from Rantin lake, Yukon, Canada. Journal of Paleolimnology 48 (1), 147–158.
Reimer, P.J., Baillie, M.G., Bard, E., Bayliss, A., Beck, J.W., Blackwell, P.G., Ramsey, C.B., Buck, C.E., Burr, G.S., Edwards, R.L., 2009. IntCal09 and Marine 09 radiocarbon age calibration curves, 0–50,000 years cal BP. Radiocarbon 51 (4), 1111–1150.
Renssen, H., Seppä, H., Heiri, O., Roche, D., Goosse, H., Fichefet, T., 2009. The spatial and temporal complexity of the Holocene thermal maximum. Nature Geoscience 2 (6), 411–414.
Rhoton, F., Smeck, N., Wilding, L., 1979. Preferential clay mineral erosion from watersheds in the Maumee river basin. Journal of Environmental Quality 8 (4), 547–550.
Robertson, P.K., Lawton, L.A., Cornish, B.J., 1999. The involvement of phycocyanin pigment in the photodecomposition of the cyanobacterial toxin, microcystin-LR. Journal of Porphyrins and Phthalocyanines 3, 544–551.
Ruffell, A., McKinley, J.M., Worden, R.H., 2002. Comparison of clay mineral stratigraphy to other proxy palaeoclimate indicators in the mesozoic of NW Europe. Philosophical Transactions of the Royal Society of London. Philosophical Transactions. Series A, Mathematical, Physical, and Engineering Sciences 360 (1793), 675–693.
Rosenberg, S.M., Walker, I.R., Mathewes, R.W., Hallett, D.J., 2004. Midge-inferred Holocene climate history of two subalpine lakes in southern British Columbia, Canada. The Holocene 14 (2), 258–271.
Sanger, J.E., 1988. Fossil pigments in paleoecology and paleolimnology. Palaeogeography, Palaeoclimatology, Palaeoecology 62 (1), 343–359.
Sanger, J.E., Crowl, G., 1979. Fossil pigments as a guide to the paleolimnology of browns lake, Ohio. Quaternary Research 11 (3), 342–352.
Sanger, J.E., Gorham, E., 1972. Stratigraphy of fossil pigments as a guide to the postglacial history of Kirchner Marsh, Minnesota. Limnology and Oceanography 17 (6), 840–854.
Schagerl, M., Donabaum, K., 2003. Patterns of major photosynthetic pigments in freshwater algae.1. 1. Cyanoprokaryota, Rhodophyta and CryptophytaAnnales de limnologieCambridge University Press, pp. 35–47.
Schagerl, M., Pichler, C., Donabaum, K., 2003. Patterns of major photosynthetic pigments in freshwater algae. 2. Dinophyta, Euglenophyta, Chlorophyceae and CharalesAnnales de limnologieCambridge University Press, pp. 49–62.
Shin, S.I., Sardeshmukh, P.D., Webb, R.S., Oglesby, R.J., Barsugli, J.J., 2006. Understanding the mid-Holocene climate. Journal of Climate 19 (12), 2801–2817.
Shinker, J.J., Bartlein, P.J., 2010. Spatial variations of effective moisture in the western United States. Geophysical Research Letters 37 (2), L02701 (1–5).
Shuman, B., Bartlein, P., Logar, N., Newby, P., Webb III, T., 2002. Parallel climate and vegetation responses to the early Holocene collapse of the Laurentide Ice Sheet. Quaternary Science Reviews 21 (16), 1793–1805.
Shuman, B., Henderson, A.K., Colman, S.M., Stone, J.R., Fritz, S.C., Stevens, L.R., Whitlock, C., 2009. Holocene lake-level trends in the Rocky Mountains, USA. Quaternary Science Reviews 28 (19), 1861–1879.
Shuman, B., Pribyl, P., Minckley, T.A., Shinker, J.J., 2010. Rapid hydrologic shifts and prolonged droughts in rocky mountain headwaters during the Holocene. Geophysical Research Letters 37 (6), L06701.
Stahl, K., Moore, R.D., Mckendry, I.G., 2006. The role of synoptic-scale circulation in the linkage between large-scale ocean–atmosphere indices and winter surface climate in British Columbia, Canada. International Journal of Climatology 26 (4), 541–560.
Steinman, B.A., Rosenmeier, M.F., Abbott, M.B., Bain, D.J., 2010a. The isotopic and hydrologic response of small, closed-basin lakes to climate forcing from predictive models: application to paleoclimate studies in the upper Columbia River basin. Limnology and Oceanography 55 (6), 2131–2145.
Steinman, B.A., Rosenmeier, M.F., Abbott, M.B., 2010b. The isotopic and hydrologic response of small, closed-basin lakes to climate forcing from predictive models: simulations of stochastic and mean-state precipitation variations. Limnology and Oceanography 55 (6), 2246–2261.
Steinman, B.A., Abbott, M.B., Mann, M.E., Stansell, N.D., Finney, B.P., 2012. 1500 year quantitative reconstruction of winter precipitation in the Pacific Northwest. Proceedings of the National Academy of Sciences of the United States of America 109, 11619–11623.
Steinman, B.A., Abbott, M.B., Mann, M.E., Ortiz, J.D., Feng, S., Pompeani, D.P., Stansell, N.D., Anderson, L., Finney, B.P., Bird, B.W., 2014. Ocean–atmosphere forcing of centennial hydroclimate variability in the Pacific Northwest. Geophysical Research Letters 47 (7), 2553–2560.
Stone, J.R., Fritz, S.C., 2006. Multidecadal drought and Holocene climate instability in the rocky mountains. Geology 34 (5), 409–412.
Sze, P., 1993. A Biology of the Algae. Wm C. Brown Publishers, p. 267.
Talbot, M., 1990. A review of the palaeohydrological interpretation of carbon and oxygen isotopic ratios in primary lacustrine carbonates. Chemical Geology: Isotope Geoscience Section 80 (4), 261–279.
Tierney, J.E., deMenocal, P.B., 2013. Abrupt shifts in Horn of Africa hydroclimate since the Last Glacial Maximum. Science 342 (6160), 843–846.
Tierney, J.E., Russell, J.M., Huang, Y., Damste, J.S., Hopmans, E.C., Cohen, A.S., 2008. Northern hemisphere controls on tropical southeast African climate during the past 60,000 years. Science (New York, N.Y.) 322 (5899), 252–255.
Toepel, J., Langner, U., Wilhelm, C., 2005. Combination of flow cytometry and single cell absorption spectroscopy to study the phytoplankton structure and to calculate the chlorophyll-a specific absorption coefficients at the taxon level1. Journal of Phycology 41, 1099–1109.
Viau, A.E., Gajewski, K., Fines, P., Atkinson, D.E., Sawada, M.C., 2002. Widespread evidence of 1500 yr climate variability in North America during the past 14,000 yr. Geology 30 (5), 455–458.
Walker, I.R., Pellatt, M.G., 2003. Climate change in coastal British Columbia—a paleoenvironmental perspective. Canadian Water Resources Journal 28 (4), 531–566.
Whitlock, C., Dean, W.E., Fritz, S.C., Stevens, L.R., Stone, J.R., Power, M.J., et al., 2012. Holocene seasonal variability inferred from multiple proxy records from Crevice Lake, Yellowstone national park, USA. Palaeogeography, Palaeoclimatology, Palaeoecology 331, 90–103.
Williams, D., 1995. Continental climate response to orbital forcing from biogenic silica records in lake Baikal. Nature 378, 769–771.
Williams, J.W., Shuman, B., Bartlein, P.J., Diffenbaugh, N.S., Webb, T., 2010. Rapid, time-transgressive, and variable responses to early Holocene midcontinental drying in North America. Geology 38 (2), 135–138.
Wilson, J.B., 1994. The 'intermediate disturbance hypothesis' of species coexistence is based on patch dynamics. New Zealand Journal of Ecology 18 (2), 176–181.
Wolfe, A.P., Vinebrooke, R.D., Michelutti, N., Rivard, B., Das, B., 2006. Experimental calibration of lake-sediment spectral reflectance to chlorophyll a concentrations: methodology and paleolimnological validation. Journal of Paleolimnology 36 (1), 91–100.
Wu, X., Kong, F., Chen, Y., Qian, X., Zhang, L., Yu, Y., et al., 2010. Horizontal distribution and transport processes of bloom-forming Microcystis in a large shallow lake (Taihu, China). Limnologica-Ecology and Management of Inland Waters 40 (1), 8–15.
Yurco, L.N., Ortiz, J.D., Polyak, L., Darby, D.A., Crawford, K.A., 2010. Clay mineral cycles identified by diffuse spectral reflectance in Quaternary sediments from the Northwind Ridge: implications for glacial–interglacial sedimentation patterns in the Arctic Ocean. Polar Research 29 (2), 176–197.